

# Exploiting CryoSat-2 altimetry for surface water monitoring and modeling

**Jiang, Liguang**

*Publication date:*
2018

*Document Version*
Publisher's PDF, also known as Version of record

# Exploiting CryoSat-2 altimetry for surface water monitoring and modeling

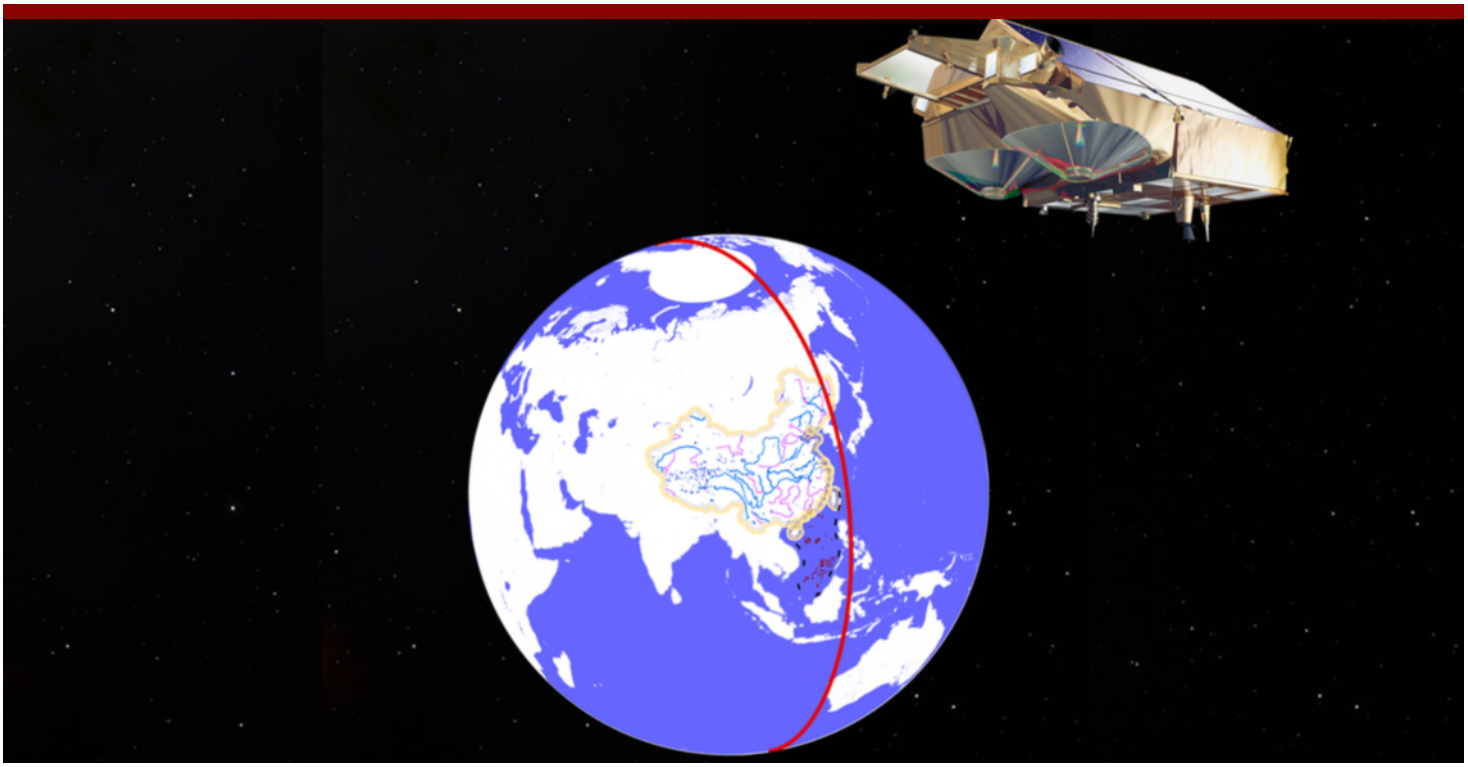

Liguang Jiang

PhD Thesis
October 2018

DTU Environment
Department of Environmental Engineering

# Exploiting CryoSat-2 altimetry for surface water monitoring and modeling

Liguang Jiang

PhD Thesis
October 2018

DTU Environment
Department of Environmental Engineering
Technical University of Denmark

**Exploiting CryoSat-2 altimetry for surface water monitoring and modeling**

**Liguang Jiang**

PhD Thesis, October 2018



Address: DTU Environment
Department of Environmental Engineering
Technical University of Denmark
Bygningstorvet, building 115
2800 Kgs. Lyngby
Denmark

Phone reception: +45 4525 1600
Fax: +45 4593 2850

Homepage: http://www.env.dtu.dk
E-mail: reception@env.dtu.dk

Cover: GraphicCo

# Preface

The work presented in this PhD thesis was conducted at the Department of Environmental Engineering of the Technical University of Denmark (DTU Environment) under the supervision of Professor Peter Bauer-Gottwein, with Senior Scientist Ole Baltazar Andersen (DTU Space) as co-supervisor. The PhD project was co-funded by the China Scholarship Council (CSC) and DTU Environment. The work was conducted from October 2015 to June 2018.

The content of the thesis is based on four scientific journal papers listed below. These papers will be referred to in the text by their paper number written with the Roman numerals **I-IV**.

**I** **Jiang, L.**, Schneider, R., Andersen, O. B., Bauer-Gottwein, P., "CryoSat-2 altimetry applications over rivers and lakes". *Water*, 2017, 9(3), 211.

**II** **Jiang, L.**, Nielsen, K., Andersen, O. B., Bauer-Gottwein, P., "Monitoring recent lake level variations on the Tibetan Plateau using CryoSat-2 SARIn mode data". *Journal of Hydrology*, 2017, 544, 109-124.

**III** **Jiang, L.**, Nielsen, K., Andersen, O. B., Bauer-Gottwein, P., "CryoSat-2 radar altimetry for monitoring freshwater resources of China". *Remote Sensing of Environment*, 2017, 200: 125-139.

**IV** **Jiang, L.**, Madsen, H., Bauer-Gottwein, P., "Calibration of river morphological parameters using satellite altimetry derived observations of water surface elevation". *In review.*

In this online version of the thesis, paper I-IV are not included but can be obtained from electronic article databases e.g. via www.orbit.dtu.dk or on request from DTU Environment, Technical University of Denmark, Bygningstorvet, Building 115, 2800 Kgs. Lyngby, Denmark, info@env.dtu.dk.

In addition, the following studies, not included in this thesis, were also conducted during this PhD study:

**V** **Jiang, L.**, Andersen, O. B., Nielsen, K., Zhang, G., Bauer-Gottwein, P., "Influence of local geoid variation and tracking problems on water surface elevation estimates derived from multi-mission altimetry for Lake Namco". In review.

**VI** **Jiang, L.**, Bauer-Gottwein, P., "How do GPM IMERG precipitation estimates perform as hydrological model forcing? Evaluation for 239 catchments across China". In preparation.

This PhD study also contributed to international conferences with the following proceeding and conference papers:

**VII** **Jiang, L.**, Madsen, H., Bauer-Gottwein, P., "Satellite altimetry-derived water level for calibration of river morphological parameters in hydrodynamic models". EGU General Assembly 2018, 9-13 April 2018, Vienna. (Oral presentation)

**VIII** **Jiang, L.**, Bauer-Gottwein, P., Nielsen, K., Andersen, O. B., "CryoSat-2 radar altimetry for monitoring surface water in China". AGU Fall Meeting 2016, 12-16 December 2016, San Francisco. (Oral presentation)

June 2018

Liguang Jiang

# Acknowledgements

First of all, I would like express my gratitude to my supervisor, Professor Peter Bauer-Gottwein. You have been such an inspiring supervisor, always willing to help and discuss. It is not possible to achieve it without your invaluable guidance, insightful comments, and considerable encouragements.

I thank my co-supervisor Senior Scientist Ole Baltazar Andersen from DTU Space for his guidance and support in the field of altimetry. It was great working with you.

I also express my thanks to Senior Researcher Karina Nielsen from DTU Space for her continued support even before I came to DTU. Thank you for many insightful discussions to handle the data sets.

I am grateful to my previous colleague Raphael Schneider, for his enthusiasm, help, and discussions not only in scientific work but also in daily life.

Thank you to the IT and administrative staff at DTU Environment for making it a great place to work.

Thank you to all of my colleagues and lunch team for making the time slot enjoyable. Special thanks to our Hydrology research group members for many meaningful discussions, Dan, Monica, Raphael, Cécile, Sheng, Filippo, Grith …

Thank you to my Chinese friends, Hailin, Zhiyong, Qingxian, Nannan … for all the good times and the help.

Last but not least, I want thank my entire family, who never stopped encouraging me in all these years. Without their support, none of this would have been possible.

"Dedicated to the memory of my mother, Fenghua Guo, who always believed in me and was constant source of inspiration to my life"

# Summary

Water shortages, floods, and droughts pose global challenges. The past decade saw severe water scarcity and flooding. The world's population continues to soar and temperature is ever rising, meaning that the freshwater we have is under severe pressure. However, we have poor knowledge of the spatial and temporal dynamics of freshwater at large scales. Remote sensing has proven useful in water resources monitoring as well as hydrological and geomorphological modeling. This is the main motivation of this research: monitoring water resources from space.

Satellite altimetry allows us to measure water surface elevation, its slope, and temporal variation. Most satellite altimetry missions (Jason series, ERS/Envisat/SARAL, etc.) have a short repeat period, i.e. 10 to 35 days while CryoSat-2 has a 369-day long repeat (geodetic orbit). However, short-repeat altimeters miss too many water bodies due to their coarse ground track spacing. Thanks to its geodetic orbit, CryoSat-2 allows a high number of water bodies to be monitored. This also provides a more highly resolved water surface elevation profile of rivers that have not been well sampled before. In the meantime, these benefits come at the cost of long repeat cycle. This particularly poses challenges to derive time series of water level at virtual stations, which are commonly used for short-repeat altimeters. Therefore, one research question is "Can we use distributed CryoSat-2 data for river modeling beyond the 'virtual station' concept?"

The contributions of this PhD project are to exploit CryoSat-2 for surface water resources monitoring in China at national scale and for hydrodynamic modeling. The aim is to understand spatiotemporal variations of freshwater resources as well as hydrodynamic modeling without precise knowledge of bathymetry.

How do lakes and reservoirs change and how can CryoSat-2 help to understand these variations? This motivates the study of water level variation of water bodies. This work demonstrates the great spatial coverage of CryoSat-2. Over 1000 lakes and reservoirs, and 6 large rivers were investigated. RMSE of CryoSat-2 over lakes is around 20 cm, and around 40 cm for most rivers, except the Yangtze and Pearl rivers. Most lakes in the Tibetan Plateau, especially those in the northern part, maintained the rising trend seen by ICESat during 2003 - 2009. Moreover, water bodies in the Junggar Basin and Huai River

Basin showed a dominant declining trend. In contrast, those in the Songnen Plain, lower Yangtze River basin showed a marked rising trend.

To understand surface water storage dynamics and its contribution to total water storage change, we estimated both surface and total water storage change by combining CryoSat-2 with water extent maps and GRACE total storage change estimates. The estimated surface water storage changes in the Tibetan Plateau, and Inner Mongolia-Xinjiang are 35.5 and $25.9\times10^8$ $m^3/yr$, respectively. On the contrary, the northeast China zone exhibited a decline. Changes in volume indicate that surface water variation contributes significantly to total storage variation, especially in the Qaidam Basin and the Tibetan Plateau, and should therefore not be omitted in land surface models.

Finally, calibration of a 1D hydrodynamic model (MIKE HYDRO River) was carried out in the Songhua River, where no bathymetry information is available. CryoSat-2 data and data from other short-repeat satellite altimeters were used to calibrate distributed river morphological parameters, i.e. roughness and river datum jointly. Clearly, CryoSat-2 by far outperforms other altimeters in both synthetic and real-world experiments. The results also show that a higher accuracy of observations does not proportionally decrease parameter uncertainty for all cross sections. Instead, high spatial sampling density (such as CryoSat-2 and Envisat) helps to identify the spatial variability of morphological parameters.

The results from this project shed light on the added value of CryoSat-2 for surface water monitoring and river modeling over China. This dataset shows the spatiotemporal variation of surface water resources at continental scale with the unique sampling pattern of CryoSat-2. This is valuable for water resource monitoring in an efficient and cost-effective way, especially for sparsely gauged or ungauged regions. Moreover, the dataset is valuable for hydrodynamic modeling considering the lack of bathymetry information for many rivers. In addition, this work is timely because the upcoming Surface Water and Ocean Topography mission will significantly improve spatial and temporal resolution of spaceborne observations of water surface elevation, and hydraulic models need to be prepared for the uptake of these data.

# Dansk sammenfatning

Vandmangel, oversvømmelse og tørke er globale udfordringer. Inden for det sidste årti findes der flere eksempler på alvorlig vandmangel, og den voksende verdensbefolkning samt stigende temperatuer øger presset på vores globale ferskvandsressourcer. Paradoksalt nok, har vi begrænset kendskab til de tidslige og rumlige dynamikker, som kontrollerer overfladevandsressourcer i stor skala. Remote sensing har vist sig at være et nyttigt redskab til overvågning af overfladevand samt til hydrologisk og geomorfologisk modellering. Det er hovedmotivationen bag dette studie: overvågning af vandressourcer fra rummet.

Altimetrisatellitter gør det muligt at overvåge overfladevandets højde og hældning samt ændringer over tid. De fleste altimetri-missioner (Jason serien, ERS/Envisat/SARAL osv.) har en kort gentagelsesperiode, d.v.s 10 til 35 dage, hvorimod CryoSat-2 har en 369 dage lang gentagelsesperiode (geodætisk bane). Desværre risikerer altimetri-missioner med korte gentagelsesperioder at misse flere vandområder, da en kortere gentagelsesperiode sker på bekostning af stor afstand imellem satellittens spor. Takket være dens geodætiske bane, kan CryoSat-2 overvåge et langt større antal vandområder. Desuden opnås en mere detaljeret profil af floder, som ellers har været sparsomt besøgt. Denne fordel medfører dog en meget lang gentagelsesperiode. Dette giver nye udfordringer, i særdeleshed i forhold til at udlede vandhøjdetidsrækker ved bestemte ”virtuelle stationer”, punkter langs floden, som missioner med korte gentagelsesperioder besøger gentagne gange. Derfor stilles problematikken: ”Kan vi anvende CryoSat-2s distribuerede data til flodmodeller ud over ”virtuelle stationer” konceptet?”

I dette PhD projekt anvendes CryoSat-2 til overvågning af overfladevandressourcer i Kina på national skala og til hydrodynamisk modellering. Formålet er at forstå variationer i ferskvandsressourcer i tid og rum, samt muligheder for hydrodynamisk modellering uden præcis kundskab til batymetri.

Hvordan ændrer søer og reservoirer sig og hvordan kan CryoSat-2 anvendes til at besvare dette spørgsmål? Dette spørgsmål er baggrunden for vores undersøgelse af vandhøjdeændringer i floder og søer. Dette studie viser CryoSat-2s bemærkelsesværdigt høje rumlige dækning. Over 1000 søer og reservoirer samt 6 store floder er undersøgt. RMSE for CryoSat-2 er omkring

20 cm for søerne og omkring 40 cm for de fleste floder, med undtagelse af Yangtze og Pearl floderne. For de fleste søer i det Tibetanske plateau – særligt i den nordlige del – fortsætter tendensen med stigende vandstand observeret af ICESat mellem 2003 og 2009. Derudover observeres en overvejende faldende tendens for vandområder i Junggar og Huai oplandene, i modsætning til den markant stigende tendens for Songnen bassinet og den nedre Yangtze flod.

Med henblik på at forstå dynamikken i overfladevandsmagasiner samt dens bridag til ændringer i den totale vandmængde, estimerer vi både ændringer i overfladevandsmagasinerne og i det totale vandlager ved at kombinere CryoSat-2 med vandareal og ændringer i den totale vandmængde målt af GRACE. Den estimerede ændring i overfladevandsmagasinet på det Tibetanske Plateau og indre Mongilia-Xinjiang er henholdsvis 35.5 og $25.9\times10^8$ $m^3$/yr. I Nordøstkina ses derimod faldende vandmængder. Ændringer i volumen indikerer at overfladevandsvariationer bidrager signifikant til ændringer i de totale vandmængder, særligt i Qaidam bassinet og det Tibetanske Plateau, og kan dermed ikke udelades fra landoverflademodeller.

I sidste del af studiet, er en 1D hydrodynamisk model (MIKE HYDRO River) kalibreret for Songhua floden, hvor ingen batymetrimålinger er tilgængelige. CryoSat-2 data, samt data fra short-repeat altimetre anvendes til kalibrering af flodens distribuerede morfologiske parametre, dvs. ruhed samt flod datum. CryoSat-2 overgår tydeligt de øvrige altimetre, både i syntetiske og virkelige eksperimenter. Resultaterne viser derudover, at højere nøjagtighed ikke sænker parameter usikkerheden proportionelt for alle tværsnit. I stedet kan den høje rumlige observationsdensitet støtte identificering af de rumlige variationer af de morfologiske parametre, som demonstreret ved brug af CryoSat-2 og Envisat data i modsætning til Jason-2 data.

Resultaterne fra dette studie kaster lys på værdien af CryoSat-2 for overflade-vandsovervågning samt -modellering i Kina. CryoSat-2s unikke overvågnings-mønster fremhæver de spatiotemporale ændringer i overfladevandsressourcer på kontintentalt plan. Dette er værdigfuldt for en effektiv og billig vandre-source overvågningsstrategi, i særdeleshed i områder med få eller ingen in-situ observationer. Derudover er hydrodynamisk modellering et værdifuldt værk-tøj, i lys af ofte mangelfulde batymetri observationer for mange floder. Dette studie er aktuelt, da den forestående Surface Water and Ocean Topography (SWOT) mission vil forbedre den spatiotemporale opløsning af rumobservati-oner af overfladevandshøjder markant. Inden da, skal hydrauliske modeller være klar til at håndtere og udnytte disse nye data.

# Table of contents

# Abbreviations

| | |
|---|---|
| 1D | 1-dimensional |
| CNES | Centre National d'Études Spatiales |
| CRPS | Continuous Ranked Probability Score |
| CS2 | CryoSat-2 |
| CTOH | Center for Topographic studies of the Ocean and Hydrosphere |
| DEM | Digital Elevation Model |
| ENV | Envisat |
| ESA | European Space Agency |
| GDR | Ground Data Record |
| GRACE | Gravity Recovery and Climate Experiment |
| HD | Hydrodynamic |
| ICESat | Ice, Cloud, and Land Elevation Satellite |
| LiDAR | Light Detection And Ranging |
| LRM | Low Resolution Mode of CryoSat-2 |
| JA1 | Jason-1 |
| JA2 | Jason-2 |
| JA3 | Jason-3 |
| LEGOS | Laboratoire d'Études en Géophysique et Océanographie Spatiales |
| RMSE | Root Mean Square Error |
| SAR | Synthetic Aperture Radar mode of CryoSat-2 |
| SARIn | Synthetic Aperture Radar Interferometric mode of CryoSat-2 |
| SD | Standard Deviation |
| SRTM | Shuttle Radar Topography Mission |
| SWOT | Surface Water and Ocean Topography |
| SWS | Surface water storage |
| TWS | Total water storage |
| WSE | Water Surface Elevation |

# 1 Introduction

## 1.1 Background and motivation

Fresh water is vital resource for life. Of all surface water on Earth, just 3% is fresh water (Dingman, 2015). Besides ice sheets, glaciers, permafrost, and groundwater, fresh water is mainly stored in reservoirs, lakes, and rivers, which provide fresh water for hundreds of millions of people, for example the Yangtze River, Yellow River, and Lake Taihu in China. However, fresh water is threatened by both climate change and intensive human activities. On the other hand, extreme events (e.g. droughts and floods) have tremendous impact on human life and property. For example, the flooding in July 2016 in China was the worst since 1998, and over 100 people died as floods occurred in Northern Provinces as well as in the Yangtze River basin. Economic costs of the floods were estimated as $33 billion (Floodlist, 2016). Understanding the information about water level (also called stage), discharge, and storage is essential for many important applications, such as flood forecasting, water resources management, engineering design, and reservoir operation among others. Therefore, there is no doubt that monitoring inland surface water is of paramount importance.

Satellite earth observation has been an alternative way to monitor surface water resources since the 1970's. Landsat imagery has been widely used to monitor water extent while other missions provide hydrologic quantities to inform hydrologic model, such as TRMM, MODIS, SMAP, GRACE, etc. (Lettenmaier et al., 2015). Among the hydrologic quantities, water level is one essential quantity in hydrological research. Conventionally, water level can be measured by reading a staff gauge, or by using instruments, such as water level data logger. Combining water level data with rating curves, discharge can be estimated. However, this approach is time-consuming and generally not used at regional scale. The need to understand fresh water resources at large scale has increased the use of satellite altimetry for measuring water level. The advantages of altimetry measurements are the global coverage and the free accessibility of the data. This facilitates the research for transboundary and inaccessible regions, such as the Brahmaputra, Zambezi, Congo, etc. During

the past two decades, satellite altimetry has been widely used in inland hydrology as more altimetry missions have become operational (Table 1).

**Table 1.** Summary of characteristics of satellite radar altimetry missions.

| Mission | Period | Frequency band | Repeat period (day) | Inter-track interval (km) | Orbit |
|---|---|---|---|---|---|
| **ERS-1** | Jul. 1991 - Mar. 2000 | Ku-band | 35 | 80 | short-repeat |
| **Topex** | Sep. 1992 - Oct. 2005 | Ku- and C-band | 10 | 315 | short-repeat |
| **ERS-2** | Apr. 1995 - Jul. 2011 | Ku-band | 10 | 315 | short-repeat |
| **GFO** | Feb. 1998 - Oct. 2008 | Ku-band | 17 | 165 | short-repeat |
| **Jason-1** | Dec. 2001 - Jun. 2013 | Ku- and C-band | 10 | 315 | short-repeat |
| **Envisat** | Mar. 2002 - Apr. 2012 | Ku- and S-band | 35 | 80 | short-repeat |
| **Jason-2** | Jun. 2008 - present | Ku- and C-band | 10 | 315 | short-repeat |
| **CryoSat-2** | Apr. 2010 - present | Ku-band | 369 | 7.5 | geodetic |
| **SARAL** | Feb. 2013 - Jun. 2016 | Ka-band | 35 | 80 | short-repeat |
| **SARAL*** | Jul. 2016 - present | Ka-band | 35 | < 40 | geodetic |
| **Jason-3** | Jan. 2016 - present | Ku- and C-band | 10 | 315 | short-repeat |
| **Sentinel-3A** | Feb. 2016 - present | Ku- and C-band | 27 | 104 | short-repeat |
| **Sentinel-3B** | Apr. 2018 - present | Ku- and C-band | 27 | 104 | short-repeat |

NB: * SARAL in drifting phase, has a virtual cycle of 35 days, therefore, the ground track does not exactly repeat over time.

In principle, satellite altimeters measure the two-way travel time of an electromagnetic pulse between water surface and antenna, and then convert it to distance (Figure 1). Different from satellite imagery, which maps the earth surface with a given pixel resolution, satellite altimetry only measures the nadir point along track. Therefore, the coverage of altimetry missions strictly depends on their ground track configuration. In most cases, altimetry has a temporal resolution of 10 - 35 days and a corresponding spatial resolution of 80 - 315 km (Table 1). One exception is CS2, which has three working modes and a very special orbit. Specifically, the radar altimetry instrument on CS2 is called SIRAL (Synthetic Aperture Interferometric Radar Altimeter). It operates in three modes, i.e. Low Resolution Mode (LRM), Synthetic Aperture mode (SAR), and Synthetic Aperture Interferometric mode (SARIn). Both SAR and SARIn modes provide finer resolution, i.e. ~ 300 m. Moreover, CS2 has a low altitude orbit, which has a finer cross-track resolution of 7.5 km at the cost of long repeat cycle of 369 days (European Space Agency and Mullar Space Science Laboratory, 2012). These characteristics make the mission valuable

for surface water monitoring. Many small lakes/reservoirs can be sampled and large ones have more observations. In addition, river WSE profiles can be well sampled and thus river morphological characteristics can be identified. This is the main motivation to exploit CS2 for inland water monitoring and modeling.

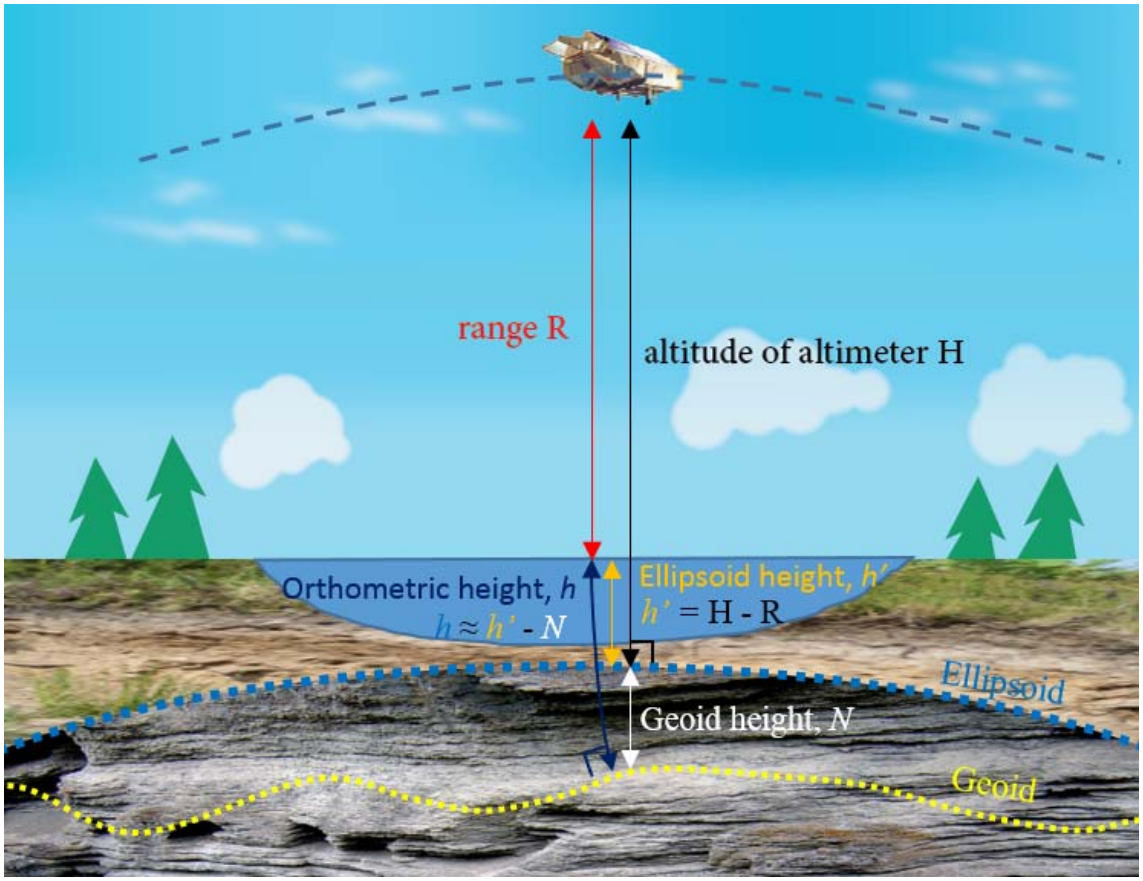


**Figure 1.** Illustration of satellite altimetry in measuring WSE. Relationship between orthometric height and ellipsoid height is illustrated. Orthometric heights mesure the distance along the curved plumb line above the geoid. Orthometrc heights depend on the earth's gratity field, and therefore better reflect what direction water will flow (Snay, 2012). Note: geoid height varies from -107 to 86 m (Pavlis et al., 2012). It is negative in most part of China.

Hydrodynamic modeling is an important tool for flood risk analysis. However, hydrodynamic modeling is challenging. One crucial procedure of hydrodynamic modeling is parameterization, which is achieved by calibration against gauged records (discharge or stage) or obtained from empirical lookup tables. On the other hand, for hydrodynamic modeling, river bathymetry is not available in many cases. These issues impede river hydraulic simulation and flood forecasting for data-sparse regions. Building a framework, which does

not heavily rely on gauging and surveying, will be valuable in data-sparse regions.

Given the coarse hydrometric monitoring network in China, it is challenging to efficiently monitoring surface water dynamics and to effectively deal with droughts and floods. These extreme events are expected to increase in frequency and magnitude under climate change as well as urbanization. Water crises not only threaten economic growth and human livelihoods, but also food security, energy security, ecosystem services, etc. (Bakker, 2012). China faces a significant challenge in maintaining water security considering the huge population and the scarcity of potable water. Therefore, monitoring and understanding of water resources using altimetry are among the motivations of this PhD project.

## 1.2 Research objectives

This PhD project attempts to solve the following research questions.

- What is the status and variations of lakes and reservoirs over the past decade? Is it measurable from satellite altimetry? And what are the linkages between lake variations and climate?
- How much surface water storage (SWS) variation contribute to the change of total water storage (TWS)? Is the contribution significant?
- Is it possible to calibrate non-uniform hydrodynamic parameters using altimetry-derived water level alone? Is the result mission-dependent?
- How to balance the tradeoff between spatial resolution (i.e. sampling configuration) and temporal resolution (repeat period) of satellite altimetry for hydrodynamic modeling?

Accordingly, this PhD project exploited the potential value of CS2 in monitoring lake dynamics, surface water distribution, and calibrating hydrodynamic river models. This synopsis answers the proposed questions and summarizes the findings. The state of the art of inland water altimetry is presented in Section 2. Data sets and study region used in this project are briefly introduced in Section 3. Later on, the main methods and procedures are given in Section 4. Consequently, results and discussion are detailed in Section 5. Finally, Sections 6 and 7 conclude the results and outlines the expected future work, respectively.

# 2 Current state of art of inland water altimetry

This chapter presents the state of the art of satellite altimetry for measuring river and lake water levels, estimating water storage, and its added value in hydrologic/hydrodynamic river modeling.

## 2.1 Monitoring of lakes

Although all satellite altimetry missions are not dedicatedly designed for inland hydrology research, altimetry has been successfully used to monitor lake level changes since the 1990's (Berry et al., 2005; Birkett, 1995; Crétaux and Birkett, 2006; Gao et al., 2013; Schneider et al., 2017; Sulistioadi et al., 2015; Villadsen et al., 2015; Zhang et al., 2011). It has recently attracted increased interest, in particular over data sparse regions.

In many cases, studies are focusing on one specific lake or a group of lakes, to investigate the water balance and the driving factors of lake changes, which is closely related to hydroclimatology. For example, lakes in the Tibetan Plateau are seen as an indicator of climate change. While most of the lakes are not gauged, altimetry has played an important role in monitoring lake level variations, and their response to climate change (Gao et al., 2013; Hwang et al., 2016; Song et al., 2015; Tseng et al., 2016; Zhang et al., 2011; Zheng et al., 2016; Zhou et al., 2013).

Different from short-repeat altimetry missions, altimeters with geodetic orbit, such as CryoSat-2 and AltiKa (since July 2016), are more useful in lake monitoring due to their high spatial sampling. Nielsen et al. (2017) studied 145 lakes with areas ranging from a few to several thousand $km^2$ in Finland, Denmark, and Canada. Paper **III** also demonstrated the extremely high coverage of CryoSat-2, which is very helpful in monitoring lakes.

## 2.2 Retrieval of discharge and storage

Discharge is one of the most important variables in hydrological sciences. However, for a long time, hydrologists rely on gauged measurements, i.e. measuring cross-sectional area A and instantaneous velocity v ($Q = Av$). Since

the end of 20th century, retrieval of discharge from space became possible (Bjerklie et al., 2005, 2003; Kouraev et al., 2004; Leon et al., 2006; Smith et al., 1996). Some of these studies relied on solely remote sensing data using power law correlation (Bjerklie et al., 2003; Smith et al., 1996) or rating curve estimated by fitting with a power law equation (Leon et al., 2006), while others based on rating curve available from survey or derived from ground-based discharge and stage (Kouraev et al., 2004).

In terms of satellite altimetry, the main approach is establishing a relationship between water level and discharge at or near a gauging station following the power law (Rantz, 1982). This method is widely applied (Getirana et al., 2009; Getirana and Peters-Lidard, 2013; Michailovsky et al., 2012). This is straightforward if there are gauged stations or existing rating curves. However, this is obviously not the case for many rivers. Some studies developed alternative method to establish rating curve for ungauged sites. For example, Birkinshaw et al. (2010) bypassed this issue by using the relationship between discharges and flow areas of two adjacent sites. Similarly, Michailovsky et al. (2012) used the relationship between discharge and the ratio of flow area and perimeter at different time for the same site. Moreover, some other algorithms are developed for the upcoming SWOT data. A summary is provided by Durand et al. (2016).

Instead of absolute water storage in a lake or river delta, it is more straightforward to estimate storage variation using satellite data. The basic idea is to calculate volume variation by the product of height change ($\Delta h$) and water extent (A), i.e. $\Delta V = \Delta h \times A$. Or more precisely, integration of small incremental volumes. For lakes, we can use following equation (Taube, 2000):

$$\Delta V = \frac{(H_{t+1} - H_t) \times \left(A_{t+1} + A_t + \sqrt{A_{t+1} \times A_t}\right)}{3} \quad (1)$$

This formula for calculating the volume of a frustum of a circular cone has been widely used by limnologists and hydrologists to compute the volume of lakes. The extents ($A_t$ and $A_{t+1}$) of water body at different dates are needed, as well as the corresponding water level (i.e. $H_t$ and $H_{t+1}$), which is usually derived from satellite imagery. Thus, an empirical relationship can also be established using the paired water level and extent (Crétaux et al., 2016). Many studies

researched the lake storage variation over the Tibetan Plateau and other regions.

Using similar techniques, storage change of inundated river delta can be calculated. For example, Becker et al. (2018) estimated water storage dynamics in Congo River combining altimetry data and GIEMS surface water extents. In a similar manner, Normandin et al. (2018) quantified water volume changes in the Mackenzie delta using altimetry and imagery.

## 2.3 Calibrating hydrodynamic model parameters

Water surface elevation is one of the most important variables in terms of flood monitoring and risk assessment. Hydrodynamic models are routinely used to compute water surface elevation and assess flood risk. One major procedure is parameterization of Manning's roughness (Bates et al., 2014), which is often calibrated or derived from a lookup table in an empirical manner. The traditional calibration is conducted at available gauging stations using Q or H. In the recent decade, satellite derived water surface elevation has been used to calibrate models. Getirana et al. (2013) investigated the benefit of using altimetry for parameterization and their results demonstrated that reasonable parameters can be obtained by using radar altimetry with competitive computational costs. Similar conclusions are also reported by Liu et al. (2015) and Domeneghetti et al. (2014).

However, a precondition is that river bathymetry is known. Obviously, it is not the case for many rivers worldwide. One routinely used solution is using topographic data (global DEM, LiDAR, etc.) or using conceptualized channel shape (e.g. triangle, rectangle, etc.) to represent river channel geometry (Wilson et al., 2007). For example, Paiva et al. (2011) parameterized a large-scale model based on SRTM DEM with rectangular cross section. Mejia et al. (2011) and Neal et al. (2015) both explored the effects of parameterized cross-sectional shapes on model performance.

Some studies explored the feasibility of calibration of bathymetry and roughness jointly. Yan et al. (2014) calibrated channel roughness and one uniform parameter to estimate channel bed elevation using Envisat altimetry data and SRTM DEM. Liu et al. (2015) took both Manning's roughness and channel geometry (5 parameters) into account for HD model calibration using both altimetry and imagery.

One of the main limitations of many previous studies is that the spatial variability of Manning's roughness is not well described. In most cases, one constant value is used for the whole studied reach. This inevitably leads to high errors and biased results, especially at non-calibrated sections. Domeneghetti et al. (2014) demonstrated that calibration of a single roughness coefficient for the whole river can be problematic. Using distributed altimetry data can be an effective solution given that river morphological characteristics can be well represented. A recent study by Schneider et al. (2018) shows that the variability of roughness coefficients can be well identified by CryoSat-2.

# 3 Case studies and data sets

## 3.1 Study areas

The Tibetan Plateau is the highest plateau in the world with an average elevation of over 4000 m, and was reputed as the 'Third Pole' and the 'Roof of the world' (Kang et al., 2010). It is well recognized that the Tibetan Plateau exerts profound influence on regional and global climate systems through thermal forcing mechanisms (Kang et al., 2010; Yanai and Li, 1994). In the meantime, the ecology and environment of the Tibetan Plateau are very sensitive to global warming and thus is seen as the 'amplifier' for global climate change (Qiu, 2008). In the recent decade, glacier retreat and lake expansion have attracted much attention. Hydrological changes, such as rises in lake level, frequent glacier lake outbursts, increased discharge resulted from glacial retreat, etc. have been the hot topics in hydrological community (Gao et al., 2012; Yang et al., 2011; Yao et al., 2012). In particular, lake variation has been widely studied through lake mapping (Lei et al., 2013; Ma et al., 2010; Yang et al., 2016). The Tibetan Plateau was used in the study of lake variations during the past decade (paper **II**).

The Songhua River is the third largest in China. It consists of 24 cities from four provinces. There is 139 000 $km^3$ agricultural land, contributing 10.6% of total grain yield of China. By 2010, the total population was 62.5 million. However, per capita GDP level is lower than the national average level. The main stem is formed by the confluence of two headwaters, i.e. the Nenjiang river and the Second Songhua River. The drainage basin is 557 000 $km^3$ and the average discharge is 2420 $m^3/s$. Precipitation occurs mainly during June to September, accounting for more than 70% of annual rainfall. Therefore, the mainstream is susceptible to flooding. Another reason to choose this river is that altimetry data quality is good and many different satellite altimetry missions have crosscuts with this river. A hydrodynamic river model was setup in the Songhua river considering data availability of both altimetry and in-situ data. Specifically, the reach between Harbin and Jiamusi is selected (Figure 2). See details in paper **IV**.

In addition, Mainland China was used to study SWS variation and to evaluate the effect of SWS on TWS change across time and space (paper **III**).

Moreover, several large rivers were also considered in the evaluation of CS2 data (paper **III**).

## 3.2 Satellite altimetry data

Currently, several projects are working on retrieval of water surface elevation of lakes and rivers from altimetry data, such as DAHITI (http://dahiti.dgfi.tum.de/en/), Theia Hydroweb (http://hydroweb.theia-land.fr/), HydroSat (http://hydrosat.gis.uni-stuttgart.de/php/index.php), etc. All these portals only provide time series instead of level-2 GDR data. Moreover, CS2 data are not available from these sites. In this project, we mainly use level 2 data from different LEGOS CTOH, CNES AVISO+, and DTU Space.

Besides retracked elevation, GRD data also includes instrument corrections, atmospheric corrections (i.e. ionospheric refraction, dry tropospheric refraction, and wet tropospheric refraction), and geophysical corrections (i.e. solid earth and pole tides).

**Table 2.** Summary of altimetry data sets used in this project.

| Mission | Recycle period (day) | Inter-track distance (km) | Time period used |
|---|---|---|---|
| **ENV** | 35 | 80 | 2007-2010 |
| **JA1** | 10 | 315 | 2007-2013 |
| **JA2** | 10 | 315 | 2008-2014 |
| **CS2** | 369 | 7.5 | 2010-2016 |
| **ICESat** | - | - | 2003-2009 |
| **AltiKa** | 35 | 80 | 2013-2016 |

As mentioned earlier, the geodetic orbit of CS2 provides very dense sampling. Figure 2 illustrates the ground tracks over the Songhua river. High sampling pattern allows monitoring more water bodies and finer river profile.

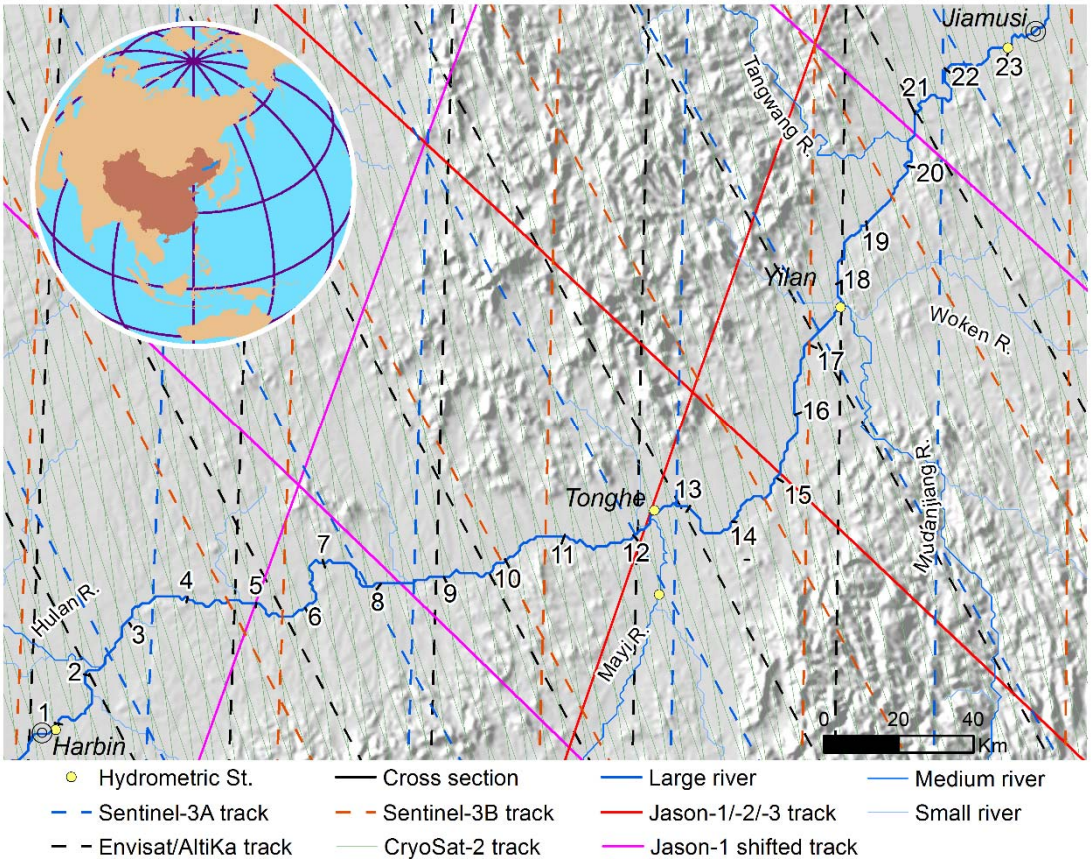


**Figure 2.** Illustration of ground sampling pattern of different altimetry missions over the Songhua River. Arabic numbers along the main stem indicate cross-sections used in hydrodynamic modeling (adapted from paper **IV**).

## 3.3 Water mask

Water mask can be retrieved from either optical images or SAR images by applying different algorithms, such as, threshold method, various water index approaches, etc. Considering the focus of this project is altimetry, our water mask is based on available products.

Currently, there are several global surface water datasets, such as the MODIS Water mask (MOD44W) (Carroll et al., 2009), SRTM Water Body Dataset (SWBD, 2003), Global Surface Water Explorer (GSWE) (Pekel et al., 2016), etc. Considering the resolution (30 m) and timeliness (1984 - 2015), GSWE was used. Specifically, water seasonality dataset was used as input, and permanent water surface mask was extracted.

## 3.4 Ancillary data

- Hydrometric data

  Daily river discharge and stage were obtained from the hydrological yearbook published by the Chinese Ministry of Water Resources. These include main stations in the Yangtze River, the Yellow River, the Pearl River, the Songhua River, and the Heilongjiang-Amur River. Water surface elevation of several lakes were also collected from the Third Pole Environment Database (http://www.en.tpedatabase.cn/ ).

- Meteorological data

  Monthly precipitation and temperature, and 30 year-averaged daily precipitation and temperature data for the Tibetan Plateau during 1985–2014 were obtained from the China Meteorological Data Service Center (http://data.cma.cn/ ). These gridded dataset at 0.5° × 0.5° spatial resolution was produced by the National Meteorological Information Center (NMIC) of the China Meteorological Administration (CMA), by interpolating observations of 2472 stations using the thin plate spline method.

  Gauged daily meteorological data including vapor pressure, relative humidity, air temperature, precipitation, wind speed, bright sunshine hours, and ground level temperature over the Songhua River basin were downloaded from the China Meteorological Data Service Center. These data were used for hydrologic modeling.

- GRACE

  GRACE data used in this research were the version RL05 L3 consisting of three solutions from the Center for Space Research, University of Texas at Austin, German Research Center for Geosciences, and Jet Propulsion Laboratory, respectively. Measurement and leakage error are also available from the same site, which is used for correction.

# 4 Methodology

## 4.1 Altimetry data editing

Level 2 GDR data contain retracked range, geophysical corrections, and satellite altitude. Therefore, water surface elevation with respect to the geoid can be calculated using the following equation:

$$H = h - R - \Delta R_{geo} - N \quad (2)$$

where, $H$ is WSE, $R$ is retracked range, $\Delta R_{geo}$ are geophysical corrections including ionosphere, wet troposphere, dry troposphere, solid earth tide, ocean loading tide, and polar tide, and $N$ is geoid height. More details can be found in papers **I** and **II**.

Because it is difficult to identify whether one return echo is from river, lake, or land solely based on waveform, especially for hydrologists, we need to compare the location of each return echo with that of a given water body. The location of a water body can be mapped from imagery as described in section 3.3. However, the extent of a water body can change with time, therefore a water mask at the exact time of altimetry observation is needed in theory. Unfortunately, such condition is hard to meet given that a satellite mission carrying both altimeter and imager is not available. A workaround is using masks collected on dates as close as those of altimetry observations (hereafter called 'dynamic mask'). We are aware that dynamic mask is more accurate to select altimetry observations. However, considering that extents of most lakes do not change dramatically, in this study, we use a static mask to select observations of water bodies. For lakes and reservoirs, data were preliminarily filtered by comparing with STRM elevation using a threshold of 20 m.

While for rivers, one track can crosscut many parts for a sinuous river. See Figure 3 below for an example from the upper Yellow river. Tracks crosscut obviously 3 reaches, which need to be treated as different parts although they have the same track number and measurement time. Therefore, a simple clustering method was applied. That is, if the distance between two consecutive observations is larger than 1 km (theoretically, it should be around 300 m), we

split this track into different groups to make sure observations of each cluster are from the same reach.

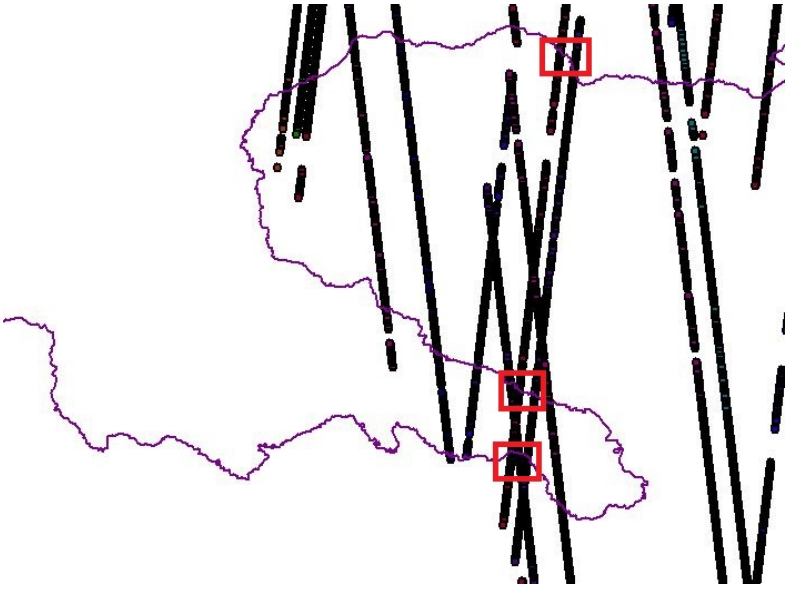

**Figure 3.** Demonstration of multiple crosscuts of ground tracks in the upper Yellow river.

## 4.2 Time series construction

Because lakes are generally wider than 300 m, there are many observations of one track at very short time slot (few seconds depending on size of a lake). Theoretically, all these observations should be of the same height. Therefore, we need to determine the height of each track. Outliers were first removed. Generally, a criterion based on mean value and standard deviation is widely used, i.e., observations should be in a range of mean ± 3 SD. Then the mean (or median) value of the remains of each track is taken as one measurement. However, this method is sensitive to outliers. In this project, a state-space model (Nielsen et al., 2015) was used for lakes. In this model, the true unobserved water surface elevation is described by a simple random walk. The model provides predictions of the evolution of the true lake water surface elevation. This considerably reduces the effect of outlying observations as shown in Figure 4. An R package (tsHydro) is available from GitHub (https://github.com/cavios/tshydro).

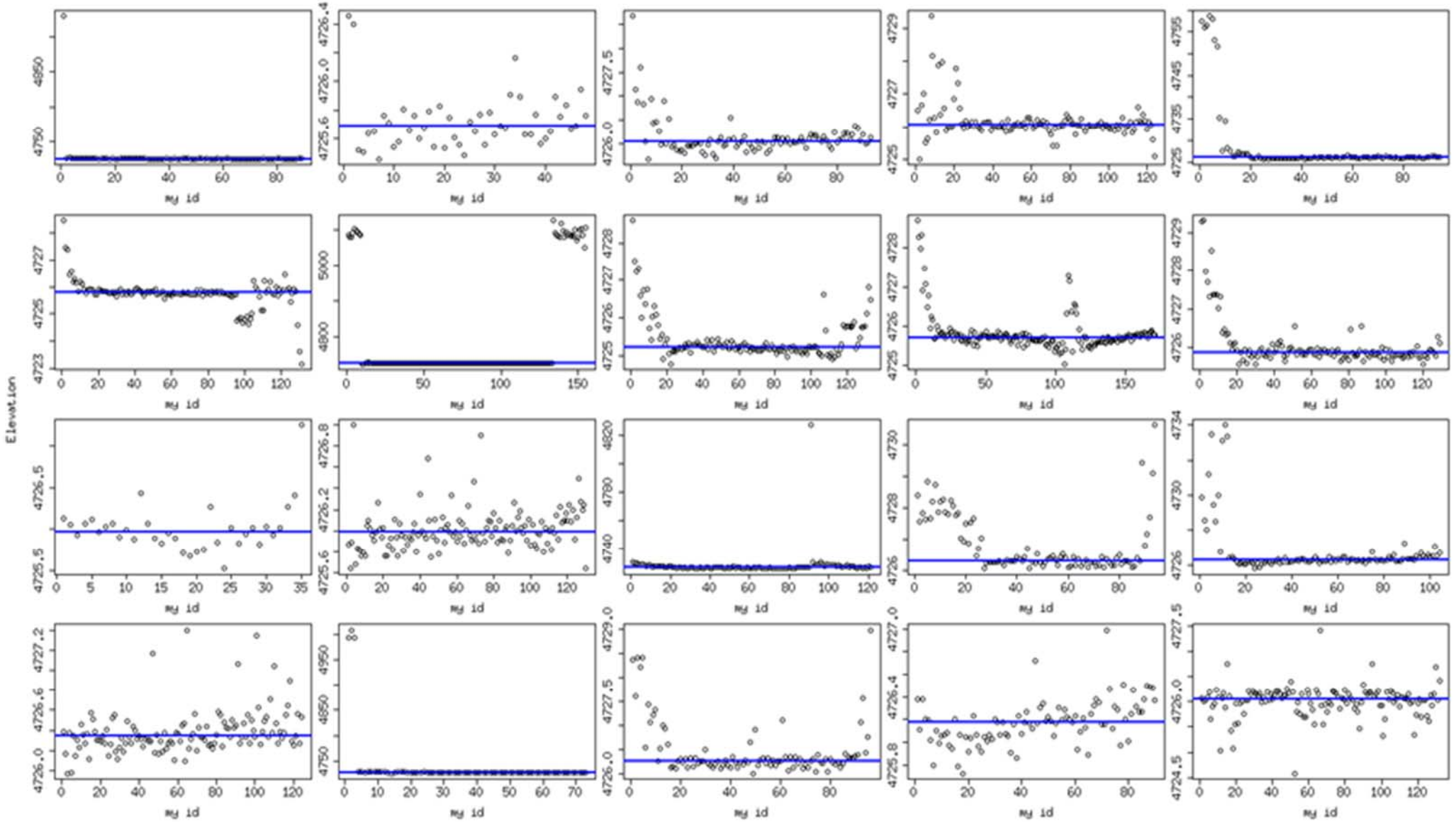


**Figure 4.** Along-track mean (blue line) and each individual (circle dot) of observations of 20 tracks over Lake Nam Co.

To evaluate data accuracy over rivers, time series at river hydrometric stations were also constructed. This was done by relocating observations to gauge station with linear interpolation based on local average slope.

## 4.3 Space-time interpolation of river longitudinal profile

The sense spatial sampling pattern of CS2 allows us to map river level variations in both space and time. The two-dimensional grid is generated by interpolation using the following procedure (Figure 5).

- For each year, a two-dimensional layer is created and each measurement is correctly setup. Therefore, seven layers in total are obtained.
- Cubic interpolation is performed to interpolate a value for void cells. Thus, a space-time map is created at resolution of 10 km by 7 days.
- For each cell point, the median value (avoid the extreme dry/wet event) from seven layers is used to generate the final map.

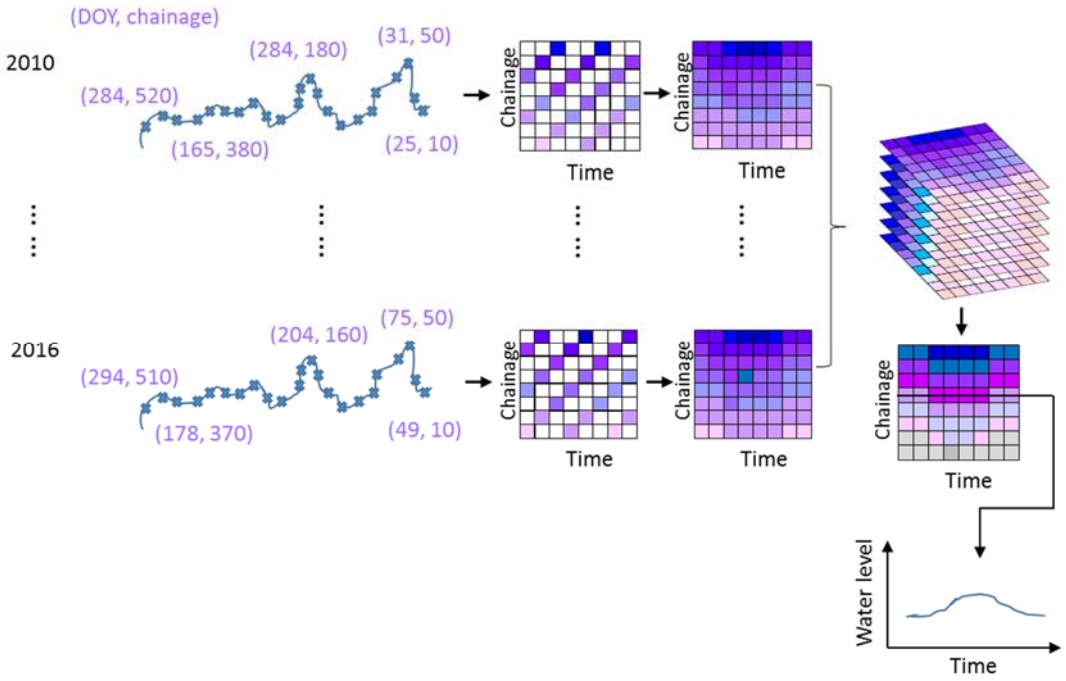


**Figure 5.** A schematic representation of the space-time interpolation of water surface elevation. The coordinate of each measurement indicates time, i.e. DOY (day of year) and chainage, i.e. location along river.

## 4.4 Water storage variation estimates

Surface water storage change estimation is based on altimetry derived water surface elevation change ($\Delta h$) and water extent ($A$). As described in section 2.2, equation (1) was used to calculate lake storage changes for the Tibetan lakes. We also compared the difference of storage estimated by using a dynamic mask and a static one. The result shows that the error induced by using a static mask is 2.5%. Due to the lack of dynamic water extent, we assume that water extent is constant during 2010 - 2016 for other lakes across China. To compare with TWS, the volume is converted to water height for hotspot regions. TWS is calculated from GRACE estimates after error correction. Refer to paper **III** for details.

## 4.5 Hydrologic-hydrodynamic Model and 1D Model Setup

Runoff from tributaries is simulated using the conceptual Xinanjiang hydrologic model, which is widely used for streamflow simulation in China (Liu et al., 2009; Zhang et al., 2012; Zhao, 1992). Besides the default 4 modules, i.e. evapotranspiration, runoff production, total runoff separation, and runoff concentration, a snow module is included to account for snow melt process. Model parameters are first calibrated against gauged discharge in 3 catchments. The optimized parameter sets are transferred to neighboring ungauged catchments.

A hydrodynamic model is set up with MIKE HYDRO River, which uses a one-dimensional simulation engine. This engine solves the Saint-Venant equations using an implicit finite-difference scheme (DHI, 2017). In this study, we use the fully dynamic Saint-Venant equation to simulate water surface elevation. River network is downloaded from HydroSHEDS dataset. The model is forced with daily discharge from upstream end, i.e. Harbin station, and normal depth is used as downstream boundary condition. Lateral inflows are either from hydrologic model outputs or 3 gauged stations.

With the aim to explore the capability of altimetry retrieved WSE to infer river bathymetry and roughness, we first conduct synthetic experiments as illustrated in Figure 6. Synthetic experiments allow us to fully explore the value of WSE data from altimetry missions. When creating synthetic altimetry

observations, two scenarios of data uncertainty are used, i.e. 20 cm and 40 cm. Basically, synthetic data are generated from one model realization, which is served as 'truth'. More details can be found in paper **IV**.

River channel is schematized as triangle and rectangle. The reason to choose these two cases it that they can be seen as end members that encompass other shapes in general. Cross sections (23 in total) are equally spaced along channel at ~ 20 km interval.

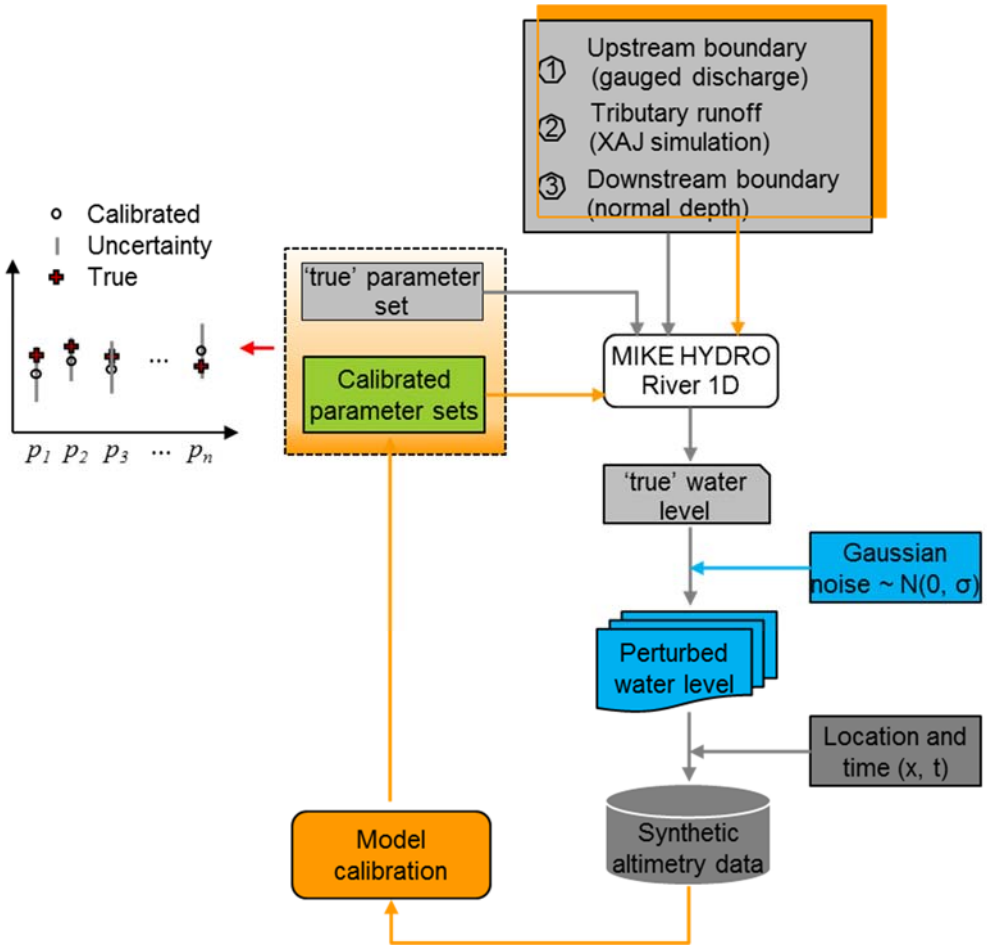


**Figure 6.** Flowchart of modeling processes. Grey arrows indicate the process of synthetic altimetry data generation, and orange ones indicate calibration process (Taken from paper **IV**).

## 4.6 Model calibration

Model calibration can be accomplished by using optimization algorithms. The hydrologic model is calibrated with genetic algorithm. The objective is to maximize the Kling-Gupta efficiency (Gupta et al., 2009).

Considering the large number of parameters (max. 3 × 23), a computationally efficient Levenberg-Marquardt (LM) algorithm is used (Marquardt, 1963). LM is widely used to solve nonlinear least squares problems. It is a combination of the gradient descent method and the Gauss-Newton method.

Inverse problems are typically ill-posed in some sense. To tackle this problem, some a priori information can be incorporated to provide an approximate solution. Regularization methods are widely used to solve such inverse problems. Regularization is typically based on differencing schemes, such as the difference of adjacent parameters. Regularization constrains are often designed to yield a smooth parameter (Tonkin and Doherty, 2005). Therefore, instead of only minimizing the mismatch of the measurements against the model outputs, regularization functions can be incorporated. That is, parameters are constrained by smoothness to facilitate inverse modeling (Pereverzyev et al., 2006).

In this study, the objective function is composed of one data fitness term and three regularization terms, i.e. smoothness of Manning's roughness coefficient, river datum, and river width (or inclination angle of triangular shape) between neighboring cross sections.

$$\min obj = \left\{ \sum_{i=1}^{Ndp} \left(H_{s,i} - H_{o,i}\right)^2 + w_1 \sum_{j=1}^{NXS} \left(Z_{j+1} - Z_j\right)^2 + w_2 \sum_{j=1}^{NXS} \left(M_{j+1} - M_j\right)^2 + w_3 \sum_{j=1}^{NXS} \left(b_{j+1} - b_j\right)^2 \right\} \quad (3)$$

where: Ndp is the total number of observations. NXS is total number of cross sections, i.e., 23. Z, M, and b are parameters to be calibrated. w is the regularization parameter (penalty) used to regularize the degree of smoothness. A strong regularization (i.e. larger w) modifies the original problem, with the advantage of leading to a smooth solution; A weak regularization (i.e. smaller w) keeps the original problem almost unchanged, but can produce wildly oscillating solutions. By adjusting these trade-off parameters, any inverse

problem can be stabilized and a unique solution can be found (Finsterle and Kowalsky, 2011).

This process is achieved by using Matlab, MIKE HYDRO River, and C#. See the flowchart below (Figure 7).

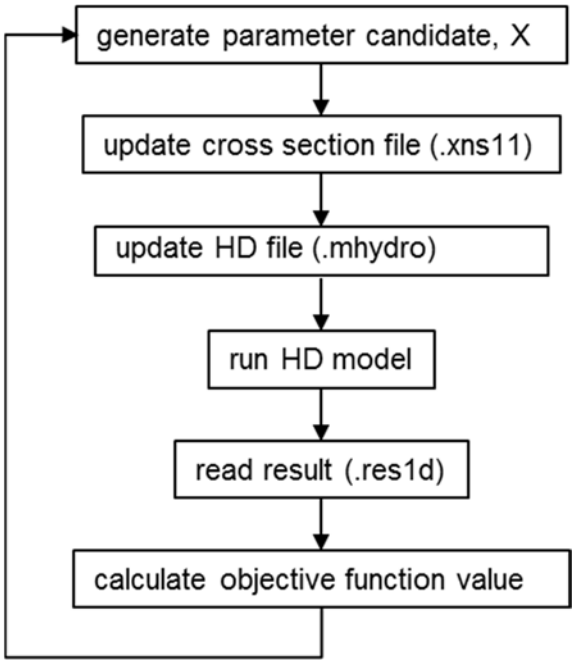


**Figure 7.** Flowchart of calibration processes. The interaction between MIKE HYDRO River and Matlab is through executable file, which is written in .NET C#.

# 5 Results and discussion

## 5.1 Variation of lake over the Tibetan Plateau

In total, 70 lakes (> 100 km$^2$) are investigated in this study. On average, these lakes are visited by CryoSat-2 34 times during the five-year period. The changing rate is depicted in Figure 8. Clearly, the majority show a significant rising trend. Specifically, 48 experienced expansion, of which 30 show significant rising trend. Interestingly, lakes with sharp increase in water surface elevation are located in the northwest and the north, i.e. groups A and B, while lakes with declining trends are mainly located in the south. However, it should be noted that most of those declining do not show a significant trend (Figure 8).

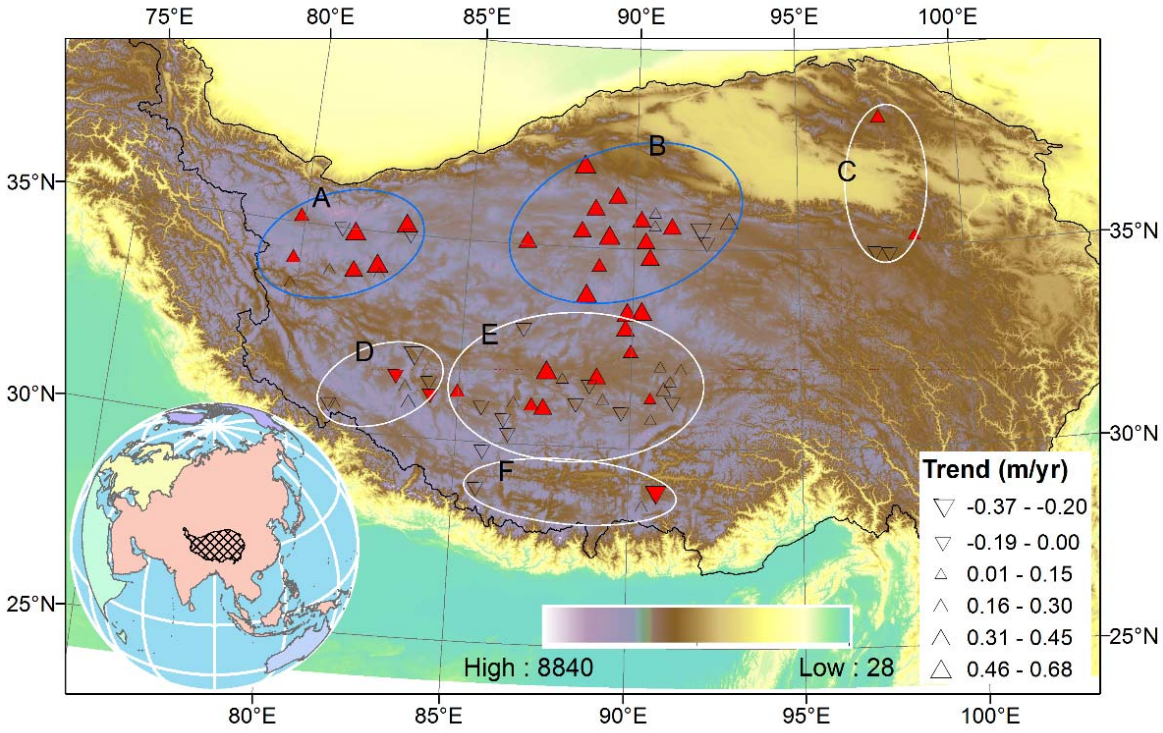


**Figure 8.** Spatial distribution of lake level changing trend. Upward/downward triangles indicate positive/negative trends. Red-coded triangles indicate significant trends at 95% confidence level (Modified from paper **II**).

Table 3 summarizes the change rate and other basin characteristics of different groups. As we can see, the average rising rates are above 0.3 m/yr for groups A and B although the climate is very cold and arid. Although the majority of shrinking lakes are from groups D and E, their declining rates are not very sharp. Overall, lake expansion is dominant for these groups except group F.

**Table 3.** Lake change statistics by sub-region and average values of basic characteristics for each sub-basin.

| Sub-region | Rising/Falling count | Avg. rising rate (m/yr) | Avg. falling rate (m/yr) | Avg. elevation (m) | Avg. precipitation (mm/yr) | Avg. temperature (°C) |
|---|---|---|---|---|---|---|
| **A** | 9/2 | 0.336 | -0.095 | 5232 | 175 | -5.01 |
| **B** | 15/2 | 0.374 | -0.142 | 4986 | 234 | -5.84 |
| **C** | 2/2 | 0.133 | -0.039 | 4415 | 266 | -0.91 |
| **D** | 3/5 | 0.155 | -0.119 | 5117 | 382 | -2.81 |
| **E** | 18/9 | 0.220 | -0.072 | 4983 | 380 | -1.79 |
| **F** | 1/2 | 0.077 | -0.227 | 5062 | 679 | -0.68 |

To look at the long-term change, we compare the recent variation with that in 2003 - 2009. Because ICESat has low spatial coverage, only 42 lakes are monitored by both ICESat and CryoSat-2. The result indicates that almost all lakes maintained rising, and the mean rising rates are comparable during the two periods (paper **II**). Figure 9 demonstrates 9 lakes with sharp increasing/decreasing trends. These lakes were rising at a rate seen by ICESat during 2003 - 2009. Most lakes had a change of 4 m or beyond 4 m. Siling Co, had a nearly 6 m rise during 12 years. On the contrary, only one lake, i.e. Yamdrok, kept significant declining.

Further, we investigated the potential influencing factors, including lake basin-wide climate normal and change rates, supply coefficient, topography, and glacier ratio, by performing regression analyses. The results indicate that lake level change rate is significantly related to annual precipitation change rate. This is straightforward, i.e. increasing precipitation resulting in more recharge to lakes. Moreover, level change rate is significantly correlated with

temperature change rates, especially in autumn and winter (Figure 10). To put it in other words, lakes are sensitive to change of cold temperature. This may be explained by permafrost thawing process, which is mainly limited by low temperature. Autumn temperature (above zero degree) rising speed the thawing of permafrost while winter temperature (below zero) rising does not melt permafrost but instead accelerates the evapotranspiration process (paper **II**). This is indicated by positive/negative correlation between level change rate and autumn/winter temperature change rate (Figure 10). More details can be found in paper **II**.

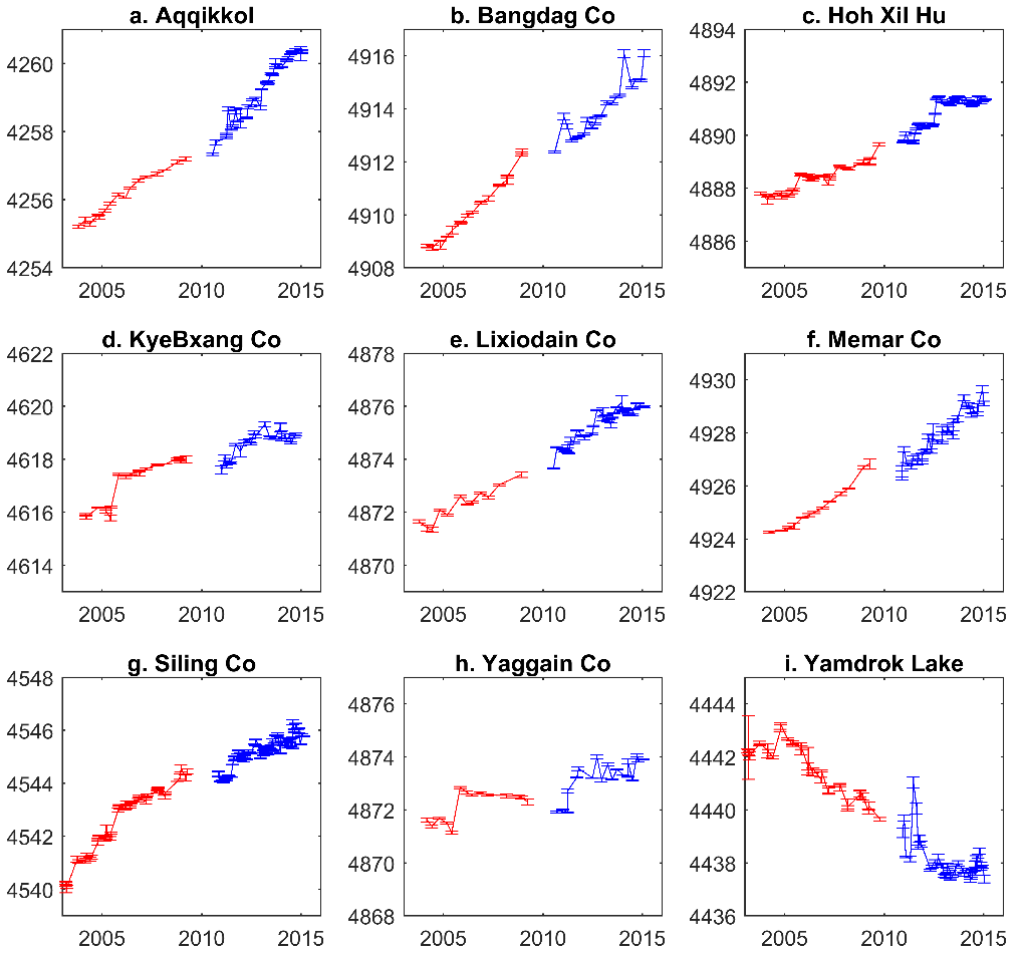


**Figure 9.** Variation of lake level between 2003 and 2015. Time series of 2003 - 2009 is derived from ICESat, and the other part from CryoSat-2, indicated by red and blue, respectively (adapted from paper **II**).

This work sheds light on variations of lakes over the Tibetan Plateau. As mentioned earlier, altimetry provides information in the vertical dimension

instead of in the horizontal dimension, in which imagery measures. Therefore, combining these two quantities allows us to quantify the water storage change, which is a very important variable in hydrological sciences. As far as we know, among serval hundred lakes over the Tibetan Plateau, water levels of most lakes are not recorded due to harsh environment and expensive costs. In this regard, satellite altimetry plays a very important role in monitoring lake variations in ungauged regions.

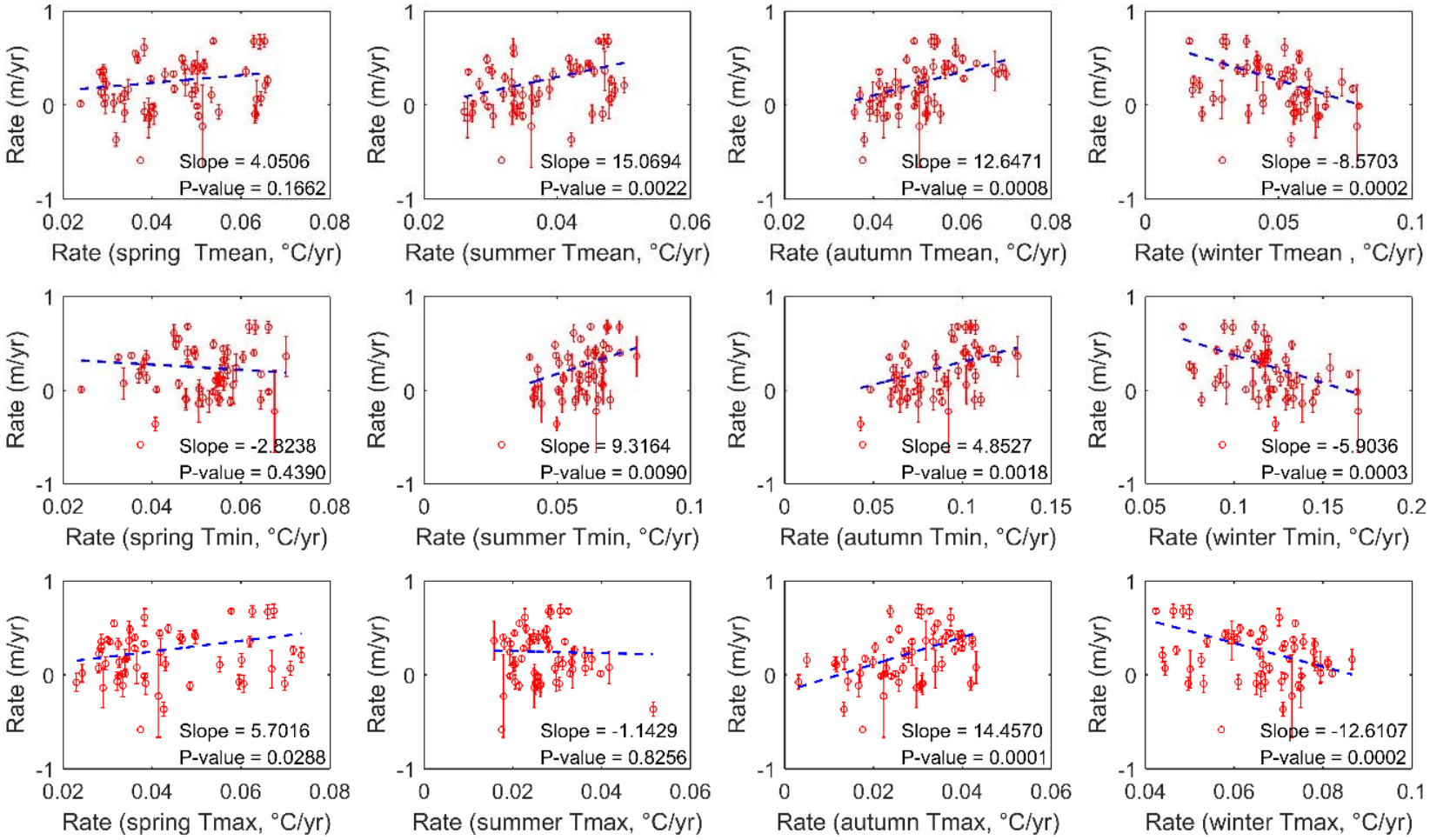


**Figure 10.** Correlation between different temperature change rate (x-axis) and lake level change rate (y-axis).

## 5.2 Surface water storage dynamics over China

Thanks to the high spatial coverage of CS2, 1334 lakes and reservoirs (> 5 $km^2$) were monitored over China during 2010 - 2016. After data editing, time series of 1163 water bodies are obtained. We can see that water surface elevation changes vary zonally, and several hotspots can be identified (Figure 11a). Specifically, water bodies located in the Junggar Basin, Huai River Basin, and Jinlin Province experienced decline, while those in Hubei Province, Songnei Plain, Qiangtang Nature Reserve had expanded. Statistically, all regions have over 50% of lakes showing expansion. Most rising lakes are located in EP and TP (Table 4).

Overall, annual amplitudes of lakes are smaller than that of reservoirs. For instance, amplitudes of lakes in the Tibetan Plateau is 0.52 ± 0.45 m on average, while reservoirs in the Yangtze River basin and Northeast Plain are larger than 5 m. This somehow makes sense because the reservoirs are heavily regulated for power generation and flood control. Moreover, annual variation of larger lakes is smaller compared to smaller ones.

Surface water storage change is quite significant in some regions, such as the North Tibetan Plateau, the lower Yangtze river basin, and Northeastern plain area (Figure 11b). As shown in Table 4, increasing rates of SWS in TP and IMX are 35.5 and 25.9 × $10^8$ $m^3$/yr, respectively. Some large lakes dominated zonal total change. For example, Hulun Lake had a storage increase rate at 15 × $10^8$ $m^3$/yr, which dominated the rate of zone IMX. Some lakes with huge storage change rate are detailed in paper III.

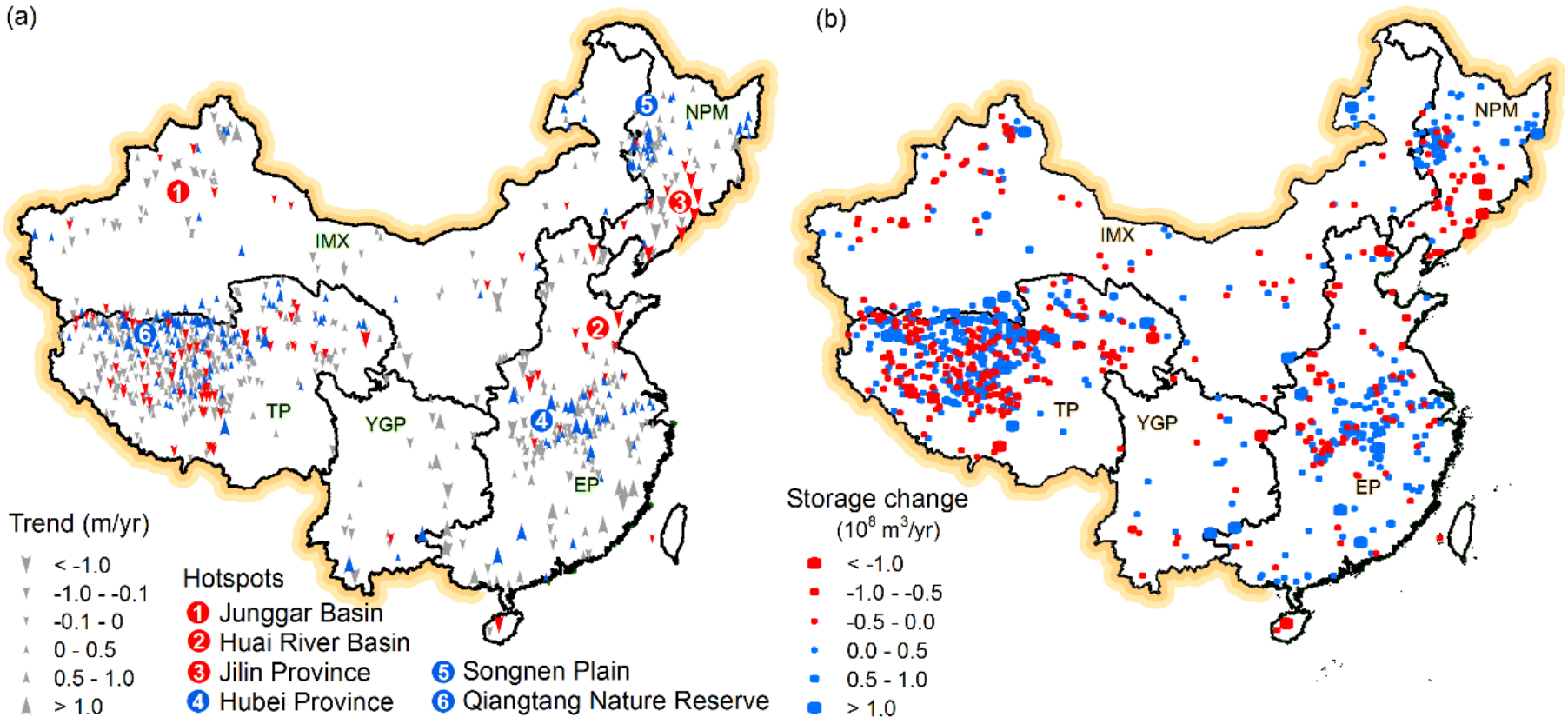


**Figure 11.** Distribution of trend (a) and storage change (b) of water bodies. Solid red and blue arrows indicate significant trends at 95% confidence level. Five zones are shown. EP is short for the Eastern Plain, IMX for Inner Mongolia and Xinjiang, NPM for Northeast Plain and Mountain, TP for the Tibetan Plateau, and YGP for Yunnan-Guizhou Plateau (Taken from paper **III**).

**Table 4.** Statistics of water surface elevation and storage changes of water bodies in five lake zones (Taken from paper **III**).

| Lake zone | Trend | Number (percentage) | Mean changing rate (m/yr) | Storage change rate ($10^8$ $m^3$/yr) |
|---|---|---|---|---|
| EP | rising | 142 (70%) | 0.330 | 9.5 ± 23.6 |
| | declining | 62 (30%) | -0.448 | |
| IMX | rising | 64 (52%) | 0.302 | 25.9 ± 24.4 |
| | declining | 58 (48%) | -0.219 | |
| NPM | rising | 60 (65%) | 0.267 | -12.4 ± 30.1 |
| | declining | 33 (35%) | -0.573 | |
| TP | rising | 247 (56%) | 0.228 | 35.5 ± 55.2 |
| | declining | 194 (44%) | -0.117 | |
| YGP | rising | 14 (61%) | 0.919 | 5.4 ± 25.4 |
| | declining | 9 (39%) | -0.592 | |

Furthermore, we investigated the influence of SWS on TWS. In general, the change rates of SWS and TWS are opposite, which indicates that the SWS increment effectively mitigates TWS loss. From a zonal perspective, the contributions of SWS to TWS are relatively small for EP and IMX, although 204 lakes and reservoirs are investigated. This is probably because these water bodies vary inhomogeneously and cancel out each other. However, SWS should be considered when evaluating groundwater variation inferred from GRACE, especially in the areas with significant SWS, such as the Tibetan Plateau and middle of the Yangtze River basin (Figure 12). Besides, reservoirs have marked impact on TWS change at national scale. More details can be found in paper **III**.

As shown in Figure 13, some hotspots can be seen as mentioned earlier. The details can be found in paper **III**. Table 5 summarizes the change rates of TWS and SWS. SWS has experienced dramatic changes and it varies regionally. On the other hand, SWS can be an important component of TWS. It should be well considered when studying groundwater variation using GRACE for example.

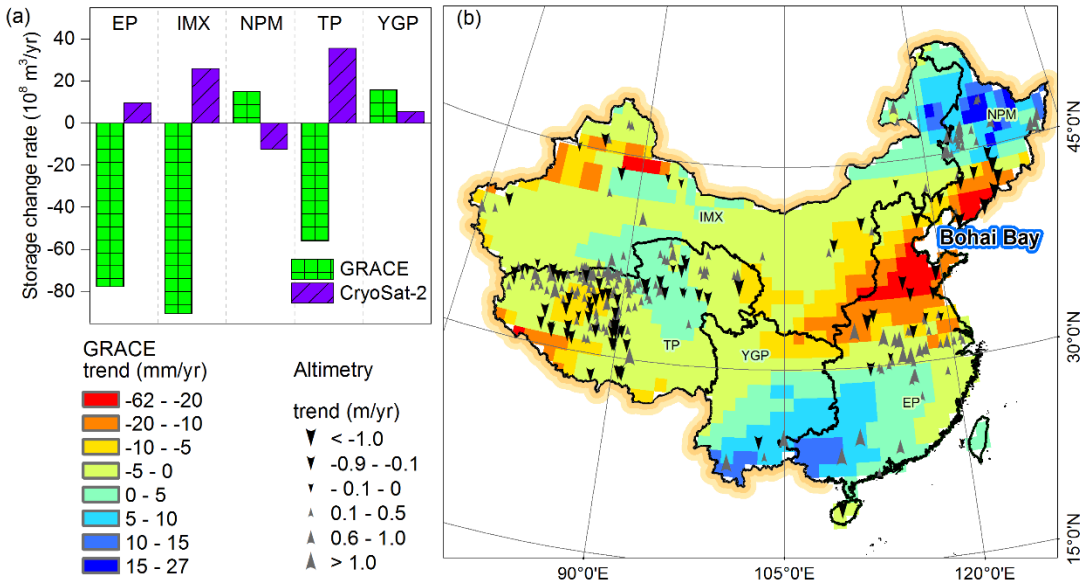


**Figure 12.** Storage change trend by zone (a) and distribution of changing trend of water surface elevation on top of TWS changing trend (b) (only 288 with significant trend shown) for the period of 2010 - 2016 (Take from paper **III**).

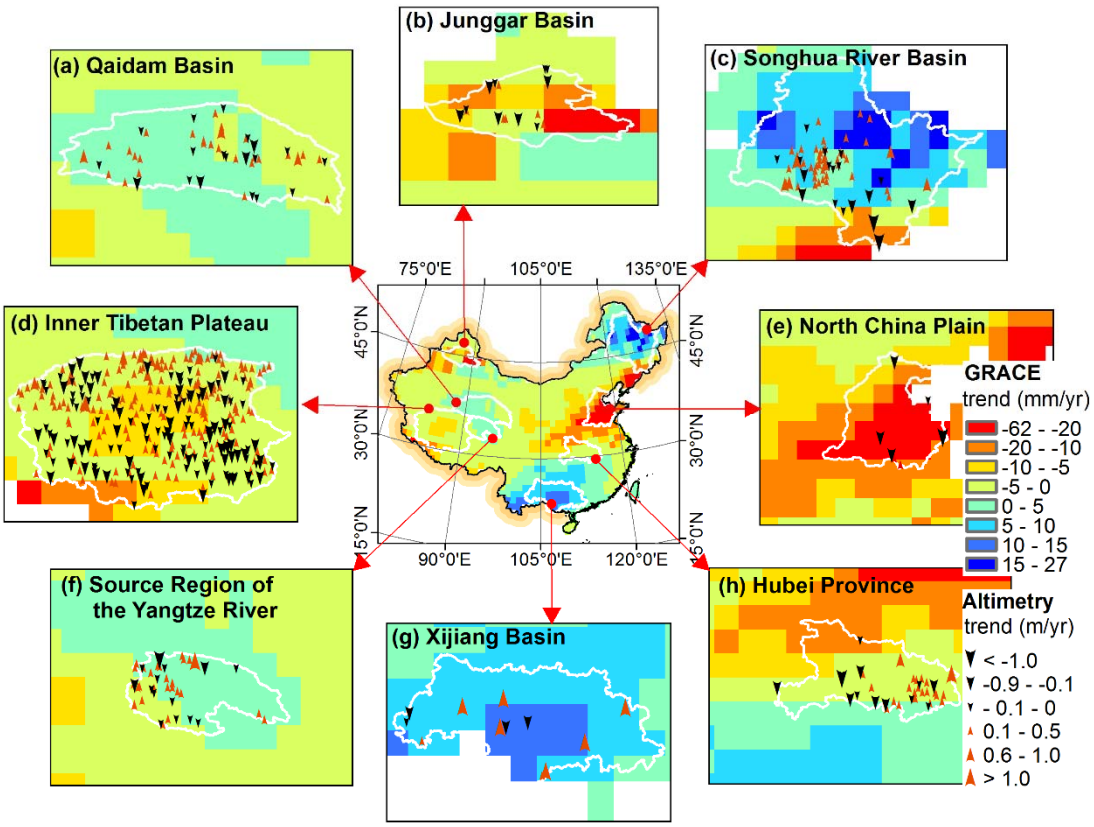


**Figure 13.** Storage change of hotspots over the period of 2010 - 2016 (Modified from paper **III**).

These regions are either ecologically fragile or face severe water shortage. Surface water is extremely important for ecosystems, especially in the western of China. In this study, we did not investigate the driving factors of surface water variation for all hotspots. However, some interesting phenomena were revealed.

Looking at the TWS of inner Tibetan Plateau, there is an abrupt increase in 2010 and since then it has declined (Figure 14d). This disagreement between TWS and SWS indicates that some components with large quantities decreased. It is probably due to the melting of glacier/snowpack. If that is the case, glacial melt must be a large quantity (- 68.9 $\times 10^8$ $m^3$/yr). Otherwise, it might be attributed to groundwater loss. However, in this complicated cryospheric region, hydrological processes are very complex, including permafrost and talik thawing/freezing, etc. Without other datasets, it is difficult to disentangle different components. More work is expected to answer this question.

The decline of TWS in North China Plain is not a surprise. As widely reported, TWS change is mainly attributed to groundwater over-exploitation. Moreover, surface water is also disturbed by intensive human activities. While TWS in the Songhua River basin shows interesting cycles. We compared TWS change with precipitation, reservoir storage change, and total water resources (Figure 15). We can see that TWS, annual precipitation, and total water resources are in good agreement. This means TWS in this region is greatly affected by precipitation.

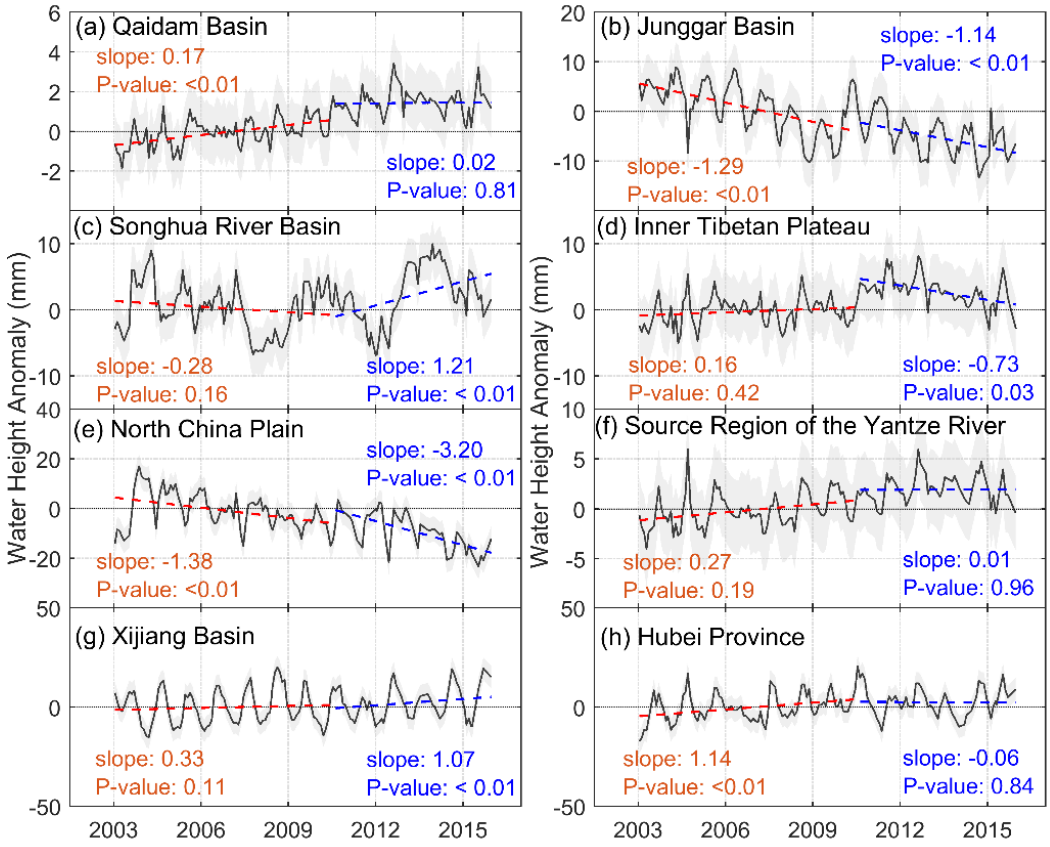


**Figure 14.** Monthly changes of TWS derived from GRACE during two periods, 2002 - 2009 and 2010 - 2016 for 8 hotspots.

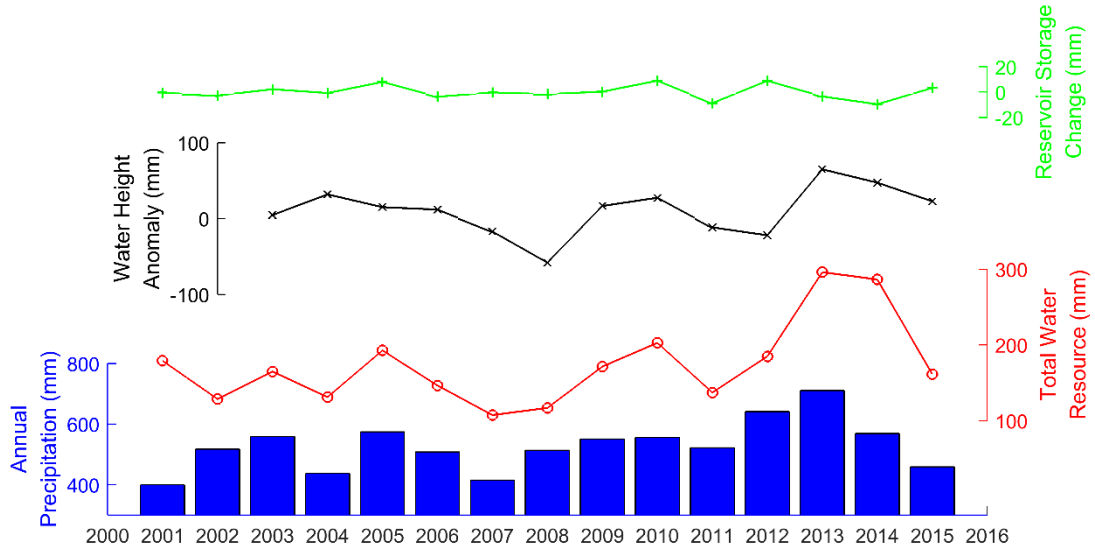


**Figure 15.** Variations of annual precipitation amount (blue bar), reservoir storage change (in green), total water resource (in red) and TWS anomaly (in black) from GRACE in Songhua River basin (from paper **III**).

**Table 5.** Statistics of TWS and SWS changes in eight hotspots during 2010 - 2016 (Units: mm/yr). Column head refers to figure 14 above.

| | a | b | c | d | e | f | g | h |
|---|---|---|---|---|---|---|---|---|
| **TWS** | 0.13 ± 0.49 | - 11.82 ± 2.41 | 6.86 ± 4.59 | - 3.14 ± 2.05 | - 20.04 ± 3.47 | 0.39 ± 1.10 | 8.65 ± 2.07 | - 5.98 ± 4.95 |
| **SWS** | 2.34 ± 1.10 | - 0.10 ± 0.53 | - 0.02 ± 2.11 | 5.09 ± 5.05 | - 0.57 ± 1.15 | 0.75 ± 1.42 | 1.72 ± 2.19 | 0.82 ± 3.71 |

## 5.3 Monitoring river water surface elevation profile

In this section, we first validated altimetry derived WSE against in-situ data over 6 Chinese rivers. Later, we demonstrated how CS2 aids to measure river longitudinal profiles. River slope can also be measured from the longitudinal profile. In the last part, we showed the great potential of CS2 to monitor river flow regimes.

### 5.3.1 Data quality over rivers

Firstly, CS2 data quality over river is validated against in-situ observations. Table 6 reports the results over 6 rivers. The results are encouraging with RMSE values ranging from 0.24 to 0.35 m for the Heilongjiang-Amur river, 0.22 to 0.6 m for the Yellow river, and 0.22 to 0.5 m for the Songhua river. Surprisingly, data quality over the two large river is very poor, i.e. RMSE around 2.6 and 3.3 m for the Yangtze and Pearl rivers. Theoretically, large rivers should have better data considering the waveform is less likely contaminated by surroundings. As shown in Table 6, RMSE is beyond 1.5 m for all virtual stations in the Yangtze river although river width is much larger than other rivers. Moreover, similar issue exists over the Pearl river (Table 6).

**Table 6.** Validation of CryoSat-2 at virtual stations against in-situ observations.

| River | Station Name | Position (km) | Mode | Width (km) | No. of measurements | RMSE (m) | $R^2$ |
|---|---|---|---|---|---|---|---|
| Yellow River | Huayuankou | 833 | LRM | ~ 1.4 | 8 | 0.25 | 0.95 |
| | Jiahetan3 | 730 | LRM | ~ 0.9 | 13 | 0.36 | 0.86 |
| | Gaocun4 | 622 | LRM | ~ 0.5 | 10 | 0.60 | 0.43 |
| | Susizhuang2 | 589 | LRM | ~ 0.5 | 12 | 0.22 | 0.96 |
| | Sunkou | 484 | Both | ~ 0.3 | 13 | 0.36 | 0.88 |
| | | | LRM | | 7 | 0.28 | 0.79 |
| | | | SARIn | | 6 | 0.41 | 0.9 |
| | huangzhuang | 444 | LRM | ~ 0.2 | 10 | 0.11 | 0.99 |
| Yangtze River | Majiadian | 1789 | LRM | ~ 1.0 | 15 | 4.02 | 0.21 |
| | Luoshan | 1454 | LRM | ~ 1.4 | 7 | 1.90 | 0.7 |
| | Hankou | 1242 | LRM | ~ 1.2 | 7 | 1.87 | 0.51 |
| | Matouzhen | 1013 | LRM | ~ 1.3 | 13 | 3.78 | 0.02 |
| | Jiujiang | 952 | LRM | ~ 2.0 | 15 | 2.84 | 0.55 |
| | Anqing | 772 | LRM | ~ 1.2 | 17 | 2.42 | 0.3 |
| | Datong2 | 685 | LRM | ~ 1.7 | 16 | 1.62 | 0.77 |
| Han River | Xiantao2 | 145 | LRM | ~ 0.3 | 5 | 0.14 | 0.99 |
| Pearl River (West R.) | Wuxuan2 | 458 | LRM | ~ 0.3 | 8 | 0.37 | 0.97 |
| | Dahuang-jiangkou2 | 362 | LRM | ~ 0.5 | 5 | 5.66 | 0.01 |
| | Pingnan | 338 | LRM | ~ 0.7 | 12 | 5.95 | < 0.01 |
| | Tengxian | 265 | LRM | ~ 0.7 | 10 | 1.16 | 0.01 |
| | Gaoyao | 42 | LRM | ~ 1.3 | 4 | 3.32 | 0.68 |
| Songhua River | Tonghe | 457 | LRM | ~ 1.1 | 13 | 0.50 | 0.31 |
| | Yilan | 354 | LRM | ~ 0.6 | 7 | 0.22 | 0.99 |
| | Fujin | 80 | LRM | ~ 1.7 | 14 | 0.30 | 0.96 |
| Heilongjiang-Amur River | Jiayin | 1535 | LRM | ~ 1.0 | 8 | 0.30 | 0.87 |
| | Luobei | 1309 | LRM | ~ 1.1 | 10 | 0.24 | 0.94 |
| | Fuyuan | 1010 | LRM | ~ 1.7 | 11 | 0.35 | 0.92 |

Further, we looked at data precision in terms of the along-track standard deviation (SD). Table 7 shows SD of water surface elevation for 6 rivers during different seasons. All rivers except Yangtze and Pearl rivers have a SD around 0.4 m. Wet season has a slightly smaller SD and SAR mode is slightly better than SRM. However, not matter in SAR or LRM mode, SDs of Yangtze and Pearl rivers are extremely high, especially in the dry season. However, as one

major tributary of the Yangtze river, Han river does not have the issue. One possible reason for this poor data quality is that waveforms are contaminated by ships using the waterway. The resulted waveform is very noisy and the retracker cannot correctly find the tracking point related to water. Previous studies over the Yangtze river also show very high uncertainty of altimetry-derived height (Sichangi et al., 2016). Another study achieved good results but the method is depending on a prior knowledge and ad hoc editing (Yuan et al., 2017). This means that a more specific retracking algorithm is needed to handle this issue for heavily navigated rivers.

**Table 7.** The precision of CryoSat-2 in terms of average of along-track standard deviation (median in bracket) (Units: m).

| River | | SD of Wet season | SD of Dry season | SD of All | SD of LRM | SD of SAR/SARIn |
|---|---|---|---|---|---|---|
| **Yellow R.** | All | 0.33 *(0.18)* | 0.40 *(0.20)* | 0.37 *(0.19)* | 0.34 *(0.18)* | SAR 0.20 *(0.09)* SARIn 0.49 *(0.32)* |
| | Upstream# | 0.35 *(0.20)* | 0.42 *(0.21)* | 0.39 *(0.21)* | | |
| | Downstream# | 0.28 *(0.14)* | 0.36 *(0.17)* | 0.32 *(0.16)* | | |
| **Yangtze R.** | All | 0.98 *(0.59)* | 1.34 *(0.90)* | 1.18 *(0.76)* | 1.33 *(0.99)* | 0.71 *(0.51)* |
| | Upstream* | 0.63 *(0.45)* | 0.77 *(0.54)* | 0.71 *(0.51)* | | |
| | Downstream* | 1.04 *(0.73)* | 1.61 *(1.30)* | 1.33 *(0.99)* | | |
| **Han R.** | | 0.38 *(0.16)* | 0.47 *(0.16)* | 0.42 *(0.16)* | 0.42 *(0.16)* | NA |
| **Pearl R.** | | 0.88 *(0.25)* | 0.90 *(0.22)* | 0.89 *(0.23)* | 0.89 *(0.23)* | NA |
| **Songhua R.** | | 0.36 *(0.16)* | 0.34 *(0.16)* | 0.35 *(0.16)* | 0.36 *(0.16)* | 0.29 *(0.13)* |
| **Heilongjiang-Amur R.** | | 0.39 (0.17) | 0.49 (0.20) | 0.45 (0.18) | 0.44 (0.18) | 0.37 (0.21) |

NA: no data available
#: Divided by the Sanmenxia Dam
*: Divided by the Three Gorges Dam

### 5.3.2 River longitudinal profile mapping

Compared with short-repeat altimeters, the key advantage of CS2 is its dense sampling pattern, which make it easier to map river longitudinal profile and thus estimate water surface slope. Figure 16 shows river longitudinal profiles and WSE changes with location. This is very promising given that no such fine river topography has been available before.

In general, CS2 delivers more measurements that are valid over rivers flowing through plain areas, and thus longitudinal profile can be well mapped, such as the case over Songhua river (Figures 16 g and h). On the contrary, CS2 is prone to miss measurements over those river parts flowing through mountainous areas, especially deep valleys, such as over upper Yangtze river. This is mainly attributed to two reasons. Firstly, when on-board tracking system works in closed-loop tracking mode, the altimeter range window is autonomously positioned and searching for signal based on on-board near-real time analysis and previous waveforms. Therefore, it will probably miss signals reflected from the river surface when topography abruptly changes (Biancamaria et al., 2017). Secondly, the echoes returning from the river surface are very weak and incoherent, which makes it difficult to retrack (Dehecq et al., 2013). To solve this problem, Jason-3 and Sentinel-3 run in open-loop tracking mode. This mode relies on the on-board digital elevation model. Some preliminary results are reported and show significant advantage of open-loop tracking over steep-sided rivers (Biancamaria et al., 2018).

Nevertheless, CS2 works well for rivers in plain regions even for narrow rivers, such as Han river (~ 300 m wide) (Figure 16). The topography is very well captured. As shown in Figure 16, the drop after the dam is clearly monitored.

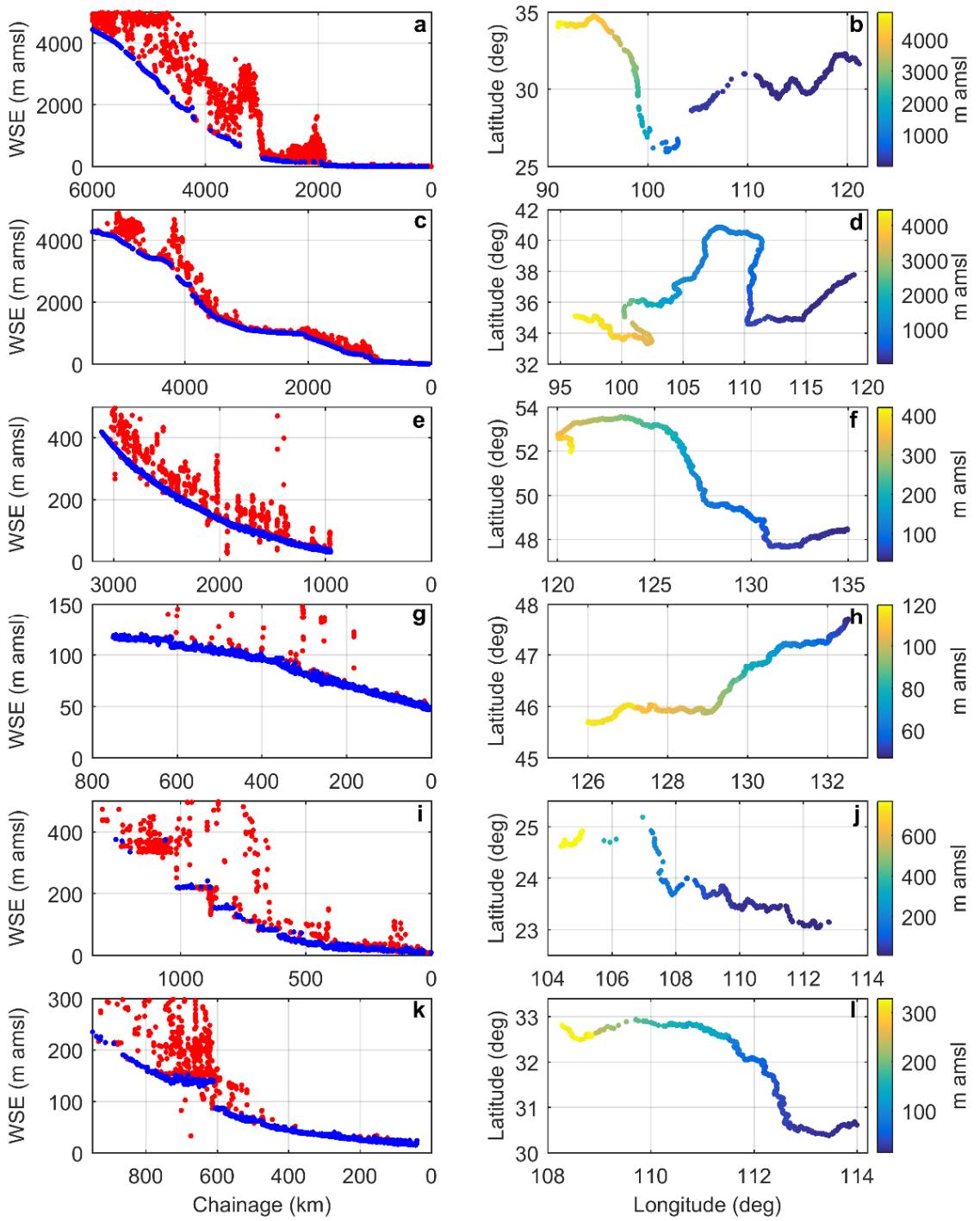


**Figure 16.** River longitudinal height profile of six rivers, a and b for the Yangtze river, c and d for the Yellow river, e and f for the Heilongjiang river, g and h for the Songhua river, i and j for the Han river, k and l for the Xijiang river. In the left column, red dots are identified as outliers by comparing with SRTM DEM.

### 5.3.3 Flow regime monitoring

The geodetic orbit allows very dense sampling of rivers in space and time. Such pattern facilitates to understand how flows are propagated along the river with time. For example, figure 17 illustrates the flow regimes of two rivers. The two-dimensional maps generally capture flow regime, peaks at around day of year 130 and 230, which correspond to spring flood (snowmelt) and summer flood (monsoon rainfall). Cross-sectional level from interpolation agrees well with in-situ water level. This is more obvious for the Heilongjiang-Amur River (Figure 17 b).

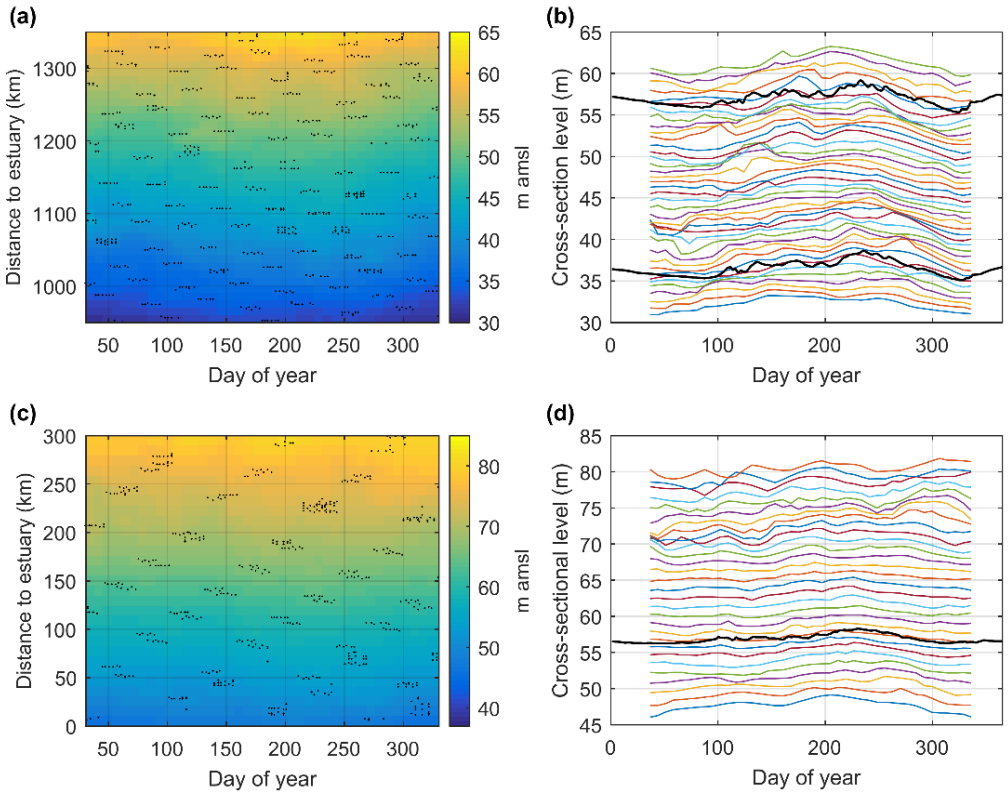


**Figure 17.** Water surface elevation maps of selected reaches of the Heilongjiang-Amur river (a and b) and the Songhua River (c and d). a and c show the space-time interpolation (CS2 measurements are dotted); b and d are water surface elevation dynamics at certain location (in-situ measurements are plotted) (From paper **III**).

## 5.4 Parameterization of 1D hydrodynamic models

### 5.4.1 Synthetic experiments

As each cross section has 3 parameters, there are a total of 7 combinations. We test all combinations to explore to what extent altimetry data can constrain these parameters. As summarized in table 8, only part of these combinations can be successfully calibration, which indicates that the 1D model cannot be calibrated using only altimetry derived SWE data. On the other hand, Manning's roughness and river datum can be jointly calibrated once inclination angle or channel width is known. This offers the opportunity to calibrate the 1D model using altimetry-derived WSE and imagery-derived river width.

**Table 8.** Summary of all synthetic experiments calibration (Taken from paper **IV**).

| NO | Triangular channel | | Rectangular channel | |
|---|---|---|---|---|
| | Combination | Successfully calibrated? | Combination | Successfully calibrated? |
| **1** | [$M$] | Yes | [$M$] | Yes |
| **2** | [$Z_0$] | Yes | [$Z_0$] | Yes |
| **3** | [$\theta$] | Yes | [$b$] | Yes |
| **4** | [$M$, $Z_0$] | Yes | [$M$, $Z_0$] | Yes |
| **5** | [$M$, $\theta$] | No | [$M$, $b$] | No |
| **6** | [$Z_0$, $\theta$] | Yes | [$Z_0$, $b$] | Yes |
| **7** | [$M$, $Z_0$, $\theta$] | No | [$M$, $Z_0$, $b$] | No |

Although combinations with two parameters can be constrained in general, different altimetry missions have various performance. Taking rectangular channel shape as an example, parameters are well recovered using CS2, i.e., calibrated parameters are much sharper using CS2 and ENV than those using JA1 and JA2. Note that all experiments use similar number of observations. This indicates spatial sampling density is much more important than temporal sampling frequency (detailed score number can be found in paper **IV**).

Another important finding is that scenario A is better than scenario B with smaller sharpness number and CRPS. However, the improvement is not proportional to data accuracy, i.e. from 40 cm to 20 cm. That means the current accuracy level is sufficient to support hydrodynamic model calibration.

Regarding individual parameters, coverage of river channel width b is relatively small. That means WSE data do not contain information of river width. Therefore, parameter b needs to be inferred from other data sources, such as imagery instead of calibration.

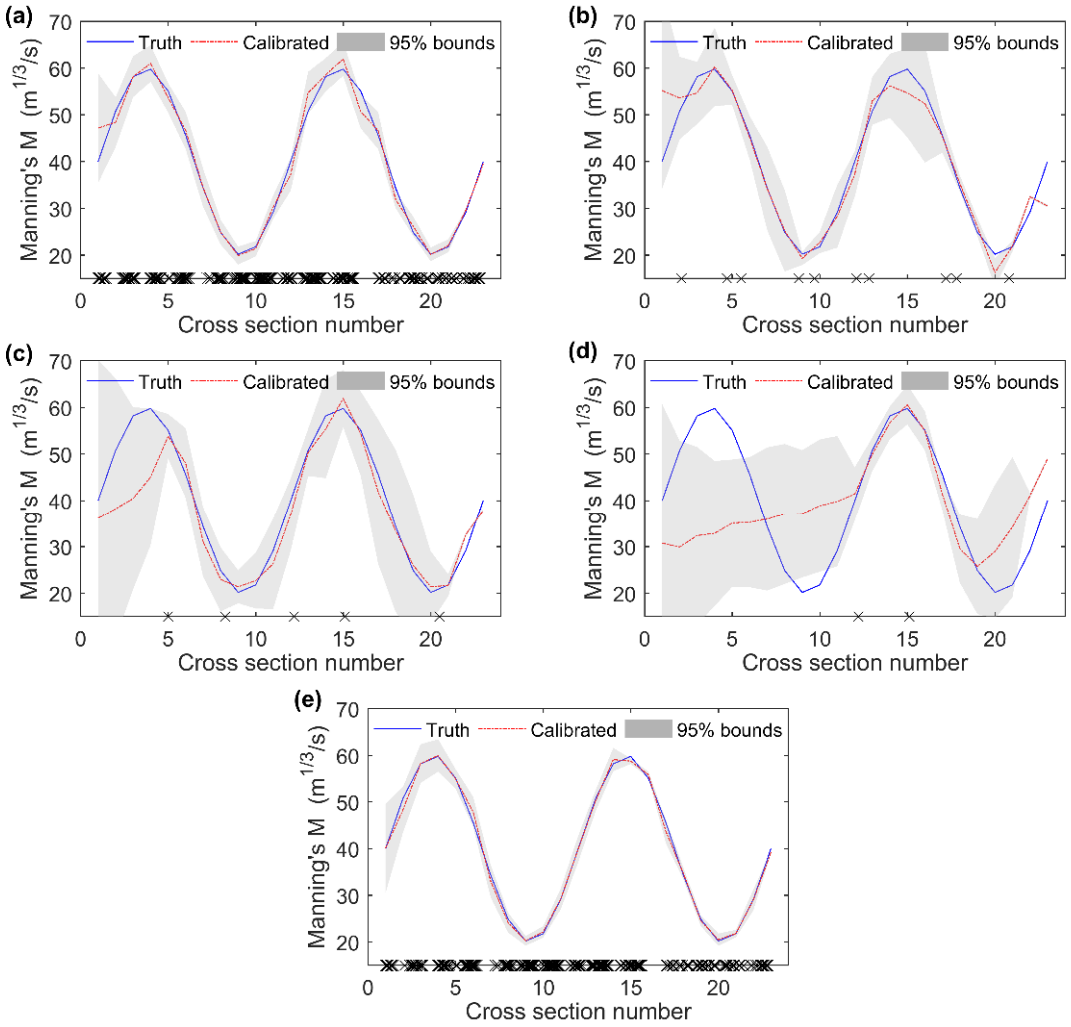


**Figure 18.** Calibration of Manning's M using synthetic data from different missions, corresponding to experiment RA1. (a) CS2; (b) ENV; (c) JA1; (d) JA2, and (e) all data. Crosses along x-axis show the nominal ground track crossing locations (From paper **IV**).

Figure 18 clearly shows spatial sampling is much important in calibrating non-uniform Manning's number. CS2 has overwhelming performance while high temporal sampling missions, i.e. JA1 and JA2, are limited to recover all parameters. Only those close to virtual stations are well calibrated. For example, at cross section numbers 12 - 17, where two virtual stations are available, parameters are recovered while others generally failed (figure 18d).

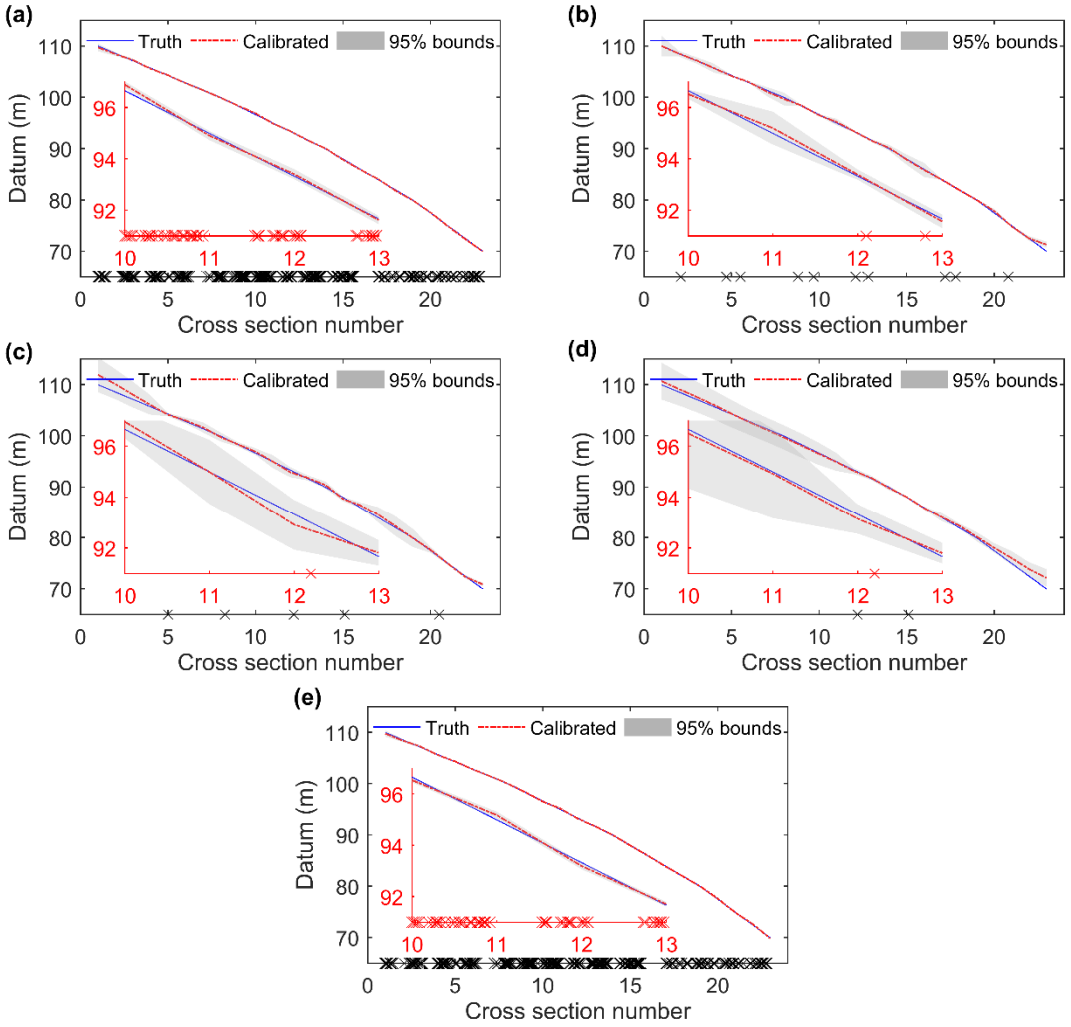


**Figure 19.** Calibration of river datum $Z_0$ using synthetic data from different missions, corresponding to experiment RA2. (a) CS2; (b) ENV; (c) JA1; (d) JA2, and (e) all data. Crosses along x-axis show the nominal ground track crossing locations (From paper **IV**).

On the other hand, even at cross sections close to virtual stations, high frequency observations do not improve sharpness. For instance, JA2 has a shorter repeat period than ENV, i.e. 10-day vs 35-day. However, the sharpness

is comparable at virtual stations (see figure 18b and 18d). Moreover, pooling all data together shows the best result. Nevertheless, CS2 alone is sufficient to constrain these non-uniform parameters.

Different from Manning's number, river datum is more directly related to altimetry observations. CS2 shows very small sharpness, i.e. 0.39 m. Other missions generally show larger uncertainty between two virtual stations due to that no observation is available to constrain parameters. Clearly, observations are insufficient to constrain parameters of cross sections, which are far away from virtual stations. Thanks to the regularization penalty, parameters of cross sections located between two virtual stations are still reasonably recovered. Similar to Manning's roughness, the datum is not well recovered in the case of JA2.

When more parameters are to be constrained, repetitive missions are incapable of recovering all parameters. As shown in Figure 20, the performance of JA-1 with five virtual stations is still acceptable. However, that of JA-2 is less satisfied even though parameters of cross sections close to virtual stations are well calibrated. This indicates that the number of virtual stations plays an important role in calibrating distributed parameters. Surprisingly, CS2 has a much longer repeat period, i.e. 369 days, but achieved very good performance.

Intuitively, it makes sense that distributed WSE is more effective to calibrate model parameters because these parameters are non-uniform and location-dependent. Spatially dense ground track can carry more information about these parameters. On the contrary, short-repeat data only sample certain sections, therefore, no information about other sections is available. While, these parameters are generally stable, and this explains why high frequency sample does not significantly improve calibration.

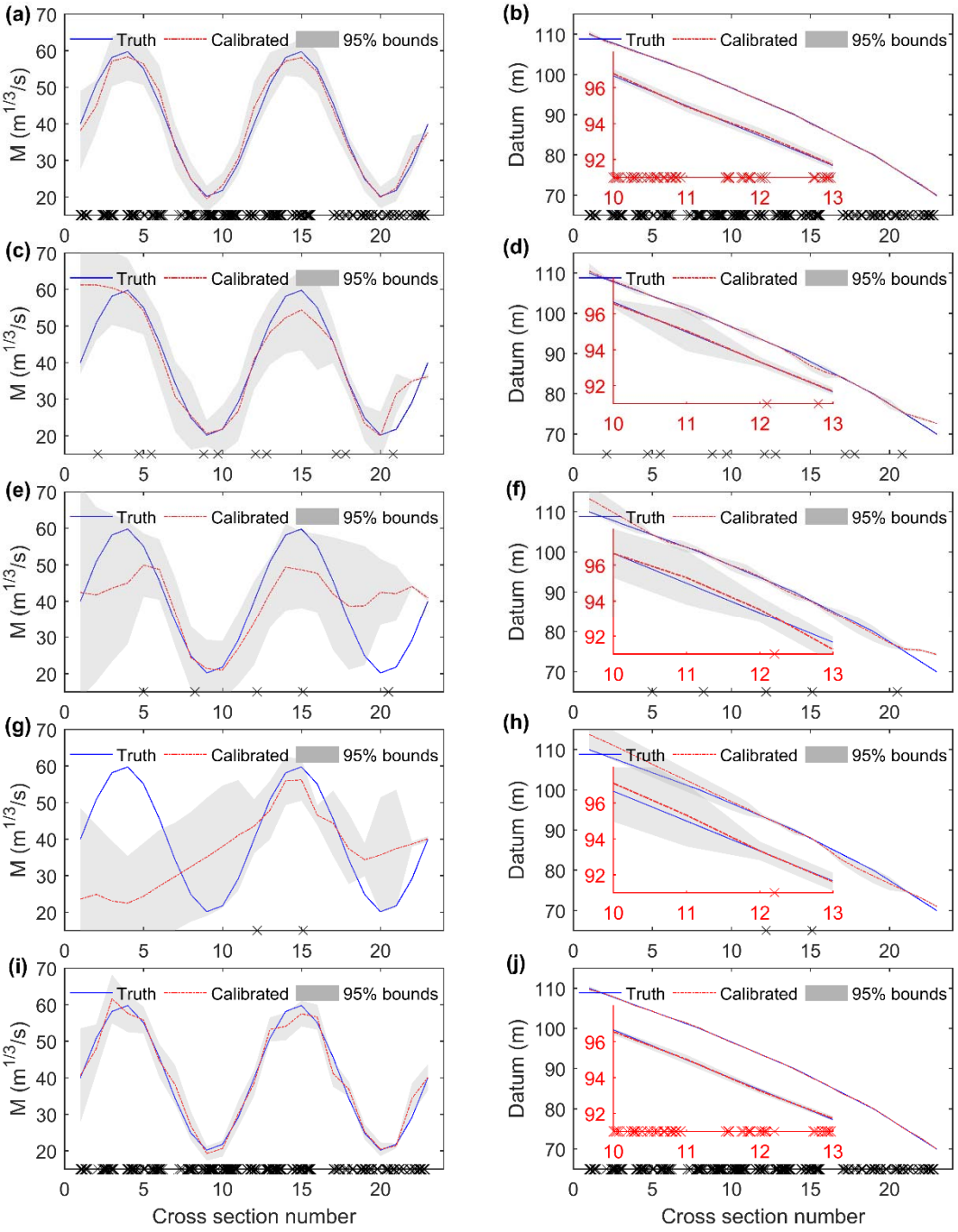


**Figure 20.** Comparison of calibrations of both Manning's number and river datum using synthetic data, corresponding to scenario RA4. Inset shows a zoomed-up plot. (a) and (b) are calibrated using CryoSat-2 data; (c) and (d) are calibrated using Envisat data; (e) and (f) are calibrated using Jason-1 data, (g) and (h) are calibrated using Jason-2 data, and (i) and (j) are calibrated using data from all missions. Crosses along the x-axis indicate the nominal VS stations (From paper **IV**).

### 5.4.2 Real-world calibration

As demonstrated in the previous section, altimetry derived WSE is incapable of constraining all three parameters. Given that the river width does not change dramatically and Songhua river is much wider, we choose rectangle to schematize channel geometry.

Model performance is summarized in Table 9. In terms of RMSE, all experiments perform fairly well. However, considering parameter sharpness, S1 and S2 are much better than other two. As expected, high spatial sampling can better constrain these parameters. S5 far outperforms others thanks to much denser sampling. It should be noted that although S2 is calibrated during 2007 - 2010, RMSE at Tonghe station is equally good as others during validation period 2010 - 2014.

**Table 9.** Summary of real-world experiments calibration (Taken from paper **IV**).

| Exper-iment | Data source | Period of data | No. of obs. | Sharpness of $M$ ($m^{1/3}/s$) | Sharpness of $Z_0$ (m) | *RMSE* [m] | | |
|---|---|---|---|---|---|---|---|---|
| | | | | | | Alt | T | Y |
| **S1** | CS2 | 2010-2014 | 261 | 52.0 | 2.59 | 1.28 | 0.33 | 0.52 |
| **S2** | ENV | 2007-2010 | 244 | 49.4 | 2.75 | 1.60 | 0.37 | 0.50 |
| **S3** | JA1 & JA2 | 2007-2014 | 319 | 45.0 | 3.19 | 0.90 | 0.35 | 0.45 |
| **S4** | JA2 | 2008-2014 | 270 | 41.1 | 4.86 | 0.72 | 0.37 | 0.44 |
| **S5** | all | 2007-2014 | 824 | 38.7 | 1.51 | 1.09 | 0.35 | 0.58 |

Alt: altimetry
T: Tonghe station, validation period: 2010 - 2014
Y: Yilan, validation period: 2007 - 2014

As spatial sampling density decreasing, the spatial variability of parameters are poorly identified. For example, the variability of M between XS 15 and 20 is not identified by Jason-1 and Jason-2 due to the lack of observations (Figures 21c and 21d). As revealed by synthetic experiments, JA2 with only two virtual stations is not sufficient to constrain these distributed parameters although it achieved satisfactory results in terms of RMSE. Similar results are shown in Figure 22 for river datum.

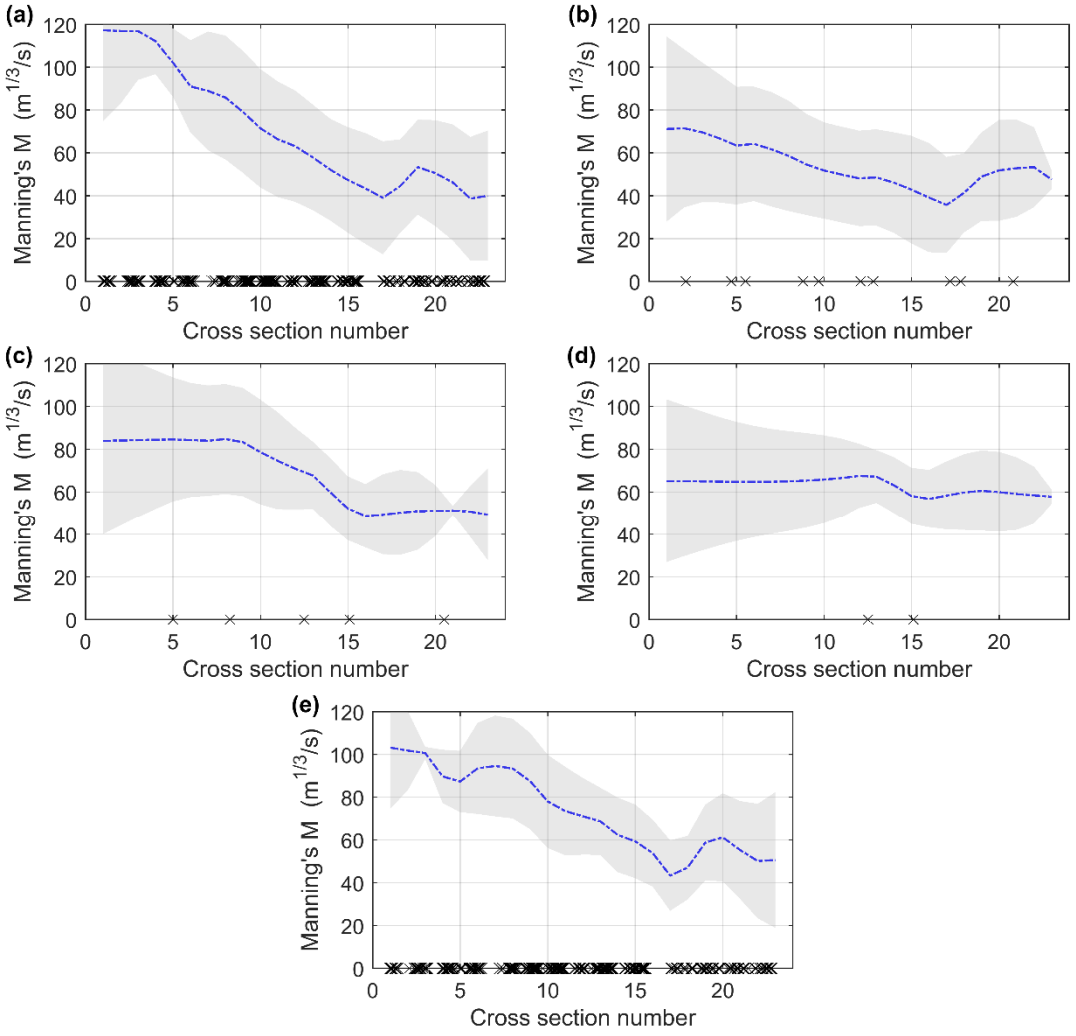


**Figure 21.** Comparison of calibrations of Manning's M using real-world observations from different altimetry missions. (a) CryoSat-2, (b) Envisat, (c) Jason-1 and Jason-2, (d) Jason-2, and (e) all missions. VS locations are indicated by crosses along the x-axis (from paper **IV**).

The results demonstrated that CryoSat-2 provides valuable information for mapping river morphological characteristics and for calibrating Manning's roughness. This is promising for poorly gauged river, even for well gauged Po River investigated by Schneider et al. (2018b). Overall, the result is promising compared with similar studies. For example, Domeneghetti et al. (2014) calibrated a quasi-2D model in the Po river against Envisat data and found a RMSE around 1 m although surveyed cross-sections were used. Our result shows better RMSE (Table 9).

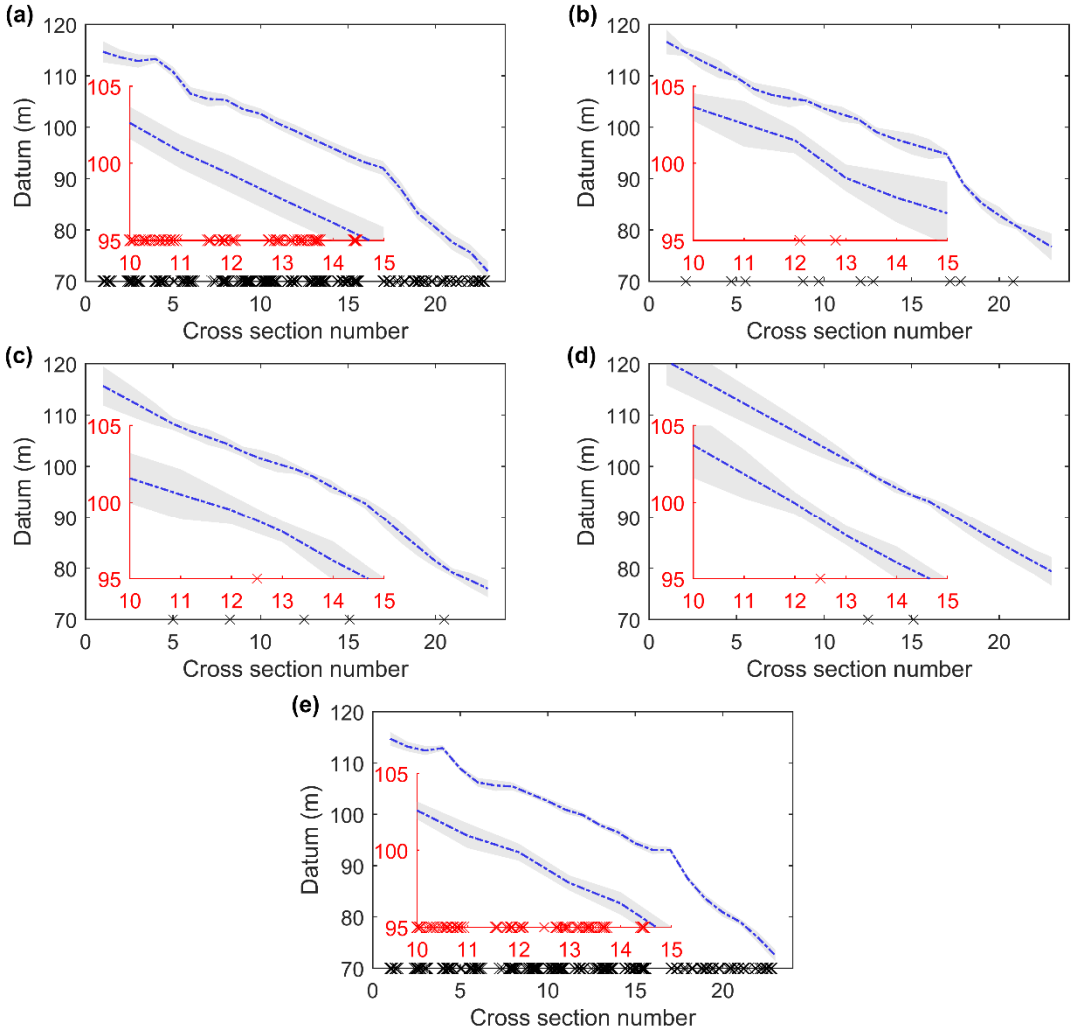


**Figure 22.** Similar to Figure 21 but for river datum (From paper **IV**).

According to our knowledge, this study is the first to study the roughness coefficient along this reach. We do not have benchmarks to validate our result although it is in a reasonable range. Meanwhile, this study can be a benchmark for future research. The underestimation of floods and overestimation of droughts (see details in paper **IV**) indicate that the conceptualized 1D model has limitations to simulate extreme events, which definitely more important. Further information concerning river morphology and physical characteristics of channel is needed to improve accuracy. This raises new questions and opens up new opportunities for hydrodynamic modeling over data-scarce rivers.

# 6 Conclusions

The overall purpose of this project is exploiting the added value of CryoSat-2 over inland water. To this end, we used CS-2 derived water surface elevation to monitor lake changes and estimate storage variations for lakes in China. Combining with GRACE, we quantified the impact of surface water storage change on total water storage variation. Moreover, we calibrated river morphological parameters over the Songhua river in China.

This is the first time that water surface elevation data are provided for over 1000 lakes and reservoirs at national scale in China. Lakes in the Tibetan Plateau have experienced marked changes during the past decade. Most of them are still rising, especially those in the northern Tibetan Plateau. A correlation analysis implies that temperature in cold seasons may play an important role in driving lake rise.

The estimated changes in water storage indicate that surface water change contribute significantly to total water storage variation, especially in the Tibetan Plateau and Qaidam Basin. This is implicative for quantification of groundwater changes using GRACE. Regarding surface water variation, some regions, such as the Junggar Basin, the Northeast China Plain, and central Yangtze river basin experienced great changes, which are mainly attributed to human activities.

This result sheds light on the status of water bodies and their variations during the past 6 years. These findings can be used as reference for eco-environmental protection and benchmark for future studies to monitor the long-term changes of inland water bodies.

Validation of CS-2 against gauged records of river stage was conducted over 6 rivers. The results are encouraging for the Heilongjiang-Amur River, the Yellow river, and the Songhua river, with RMSE ranging from 0.2 m to 0.6 m. It also indicates that CS2 is able to monitor middle-sized rivers, such as the Han River with RMSE of 0.14 m.

The value of water surface elevation for calibration of non-uniform morphological parameters is demonstrated over the Songhua River. Compared with short-repeat altimeters, CryoSat-2 shows overwhelming advantages due to its dense sampling pattern. Envisat achieved a satisfactory result with 10

virtual stations, whereas combined JA1 and JA2 constrained the parameters to a lesser extent. However, JA2 alone cannot identify the morphological characteristics with only two virtual stations. The findings clearly show that spatial sampling density is much more important than temporal sampling frequency. CS2 is able to calibrate roughness coefficient and river datum jointly, which is not achievable using short-repeat missions, such as JA2. This is promising in the sense of not requiring bathymetry data, and the approach can be used for other poorly gauged rivers.

The work conducted in this PhD project is important for understanding surface water dynamics in China, but also clearly demonstrates the added value of CS2 in supporting calibration of distributed morphological parameters. Especially in data sparse regions, CS2 will be of great value for water monitoring and river modeling.

# 7 Future perspectives

Recent advances of earth observation allow us to better monitor water resources and understand hydrological processes. Inland water altimetry, measuring water bodies in the vertical dimension, poses great opportunities and challenges, as more missions will be/are in operation. Below are some thoughts about future perspectives of inland water altimetry.

**a. Short-repeat orbit vs geodetic orbit**

One of the key features of CS2 is its geodetic orbit, which has a 30-day sub-cycle and a 369-day full repeat cycle (Wingham et al., 2006). The obvious advantage is the high-density coverage, which allows more water bodies to be observed than other missions (paper **III**). It greatly improves our understanding of lake variations of both large lakes and small ones. The main challenge is construction of time series, especially for rivers in the context of 'virtual stations'. However, beyond the concept of 'virtual stations', it is invaluable in hydrodynamic model calibration and forecasting. Similar to the concept of hydrological model calibration using multi-site observed data, distributed WSE from CS2 provides more information about river morphological characteristics. This is demonstrated in paper **IV** and Schneider et al. (Schneider et al., 2018a, 2018b). Instead of geodetic orbit, a constellation of satellite altimeters can also deliver dense samplings, such as the newly launched Sentinel-3 twins, of which the ground inter-track spacing is around 50 km and repeat period is 27 days. Considering ENV can effectively constrain model parameters to some extent, Sentinel-3 should have much better performance given that they have the same repeat cycle. The future SWOT mission will also facilitate river monitoring and modeling by delivering high spatial stage, slope and width twice roughly every 21 days (Biancamaria et al., 2016). In this context, updating hydrodynamic models using CS2-derived water surface elevation deserves more attention.

**b. Narrow river modeling**

So far, most studies of informing river modelling with altimetry are carried out in large river basins, such as Amazon river basin, Congo river basin, Zambezi river basin, Ganga-Brahmaputra river basin, etc. This is mainly due to data quality deterioration over narrow rivers. However, with SAR mode,

CS2 has been successfully applied over medium-sized rivers, such as the Po river, which is around 200 - 300 m wide (Schneider et al., 2018b). In addition, as investigated in this work, the Han River (~ 300 m wide) is well monitored even though it is in LRM mode. For even narrower rivers, the number of observations will definitely decrease. It should be interesting to investigate the potential of CS2 for narrower river even though the number of observations is not high. A data assimilation framework developed by Schneider et al. (Schneider et al., 2018a) can be applied to investigate this issue. Similar to CS2, SARAL/AltiKa is on a geodetic orbit since July 2016. The orbit has a virtual "cycle" duration of 35 days (1002 passes with ~ 16-day subcycle) (CNES, 2016). This offers us opportunity to investigate much narrower rivers due to its Ka-band.

Moreover, monitoring small rivers can benefit from advanced measuring techniques. For example, altimeters working in Ka-band, such as SARAL/AltiKa, can improve data quality. Besides, altimeters operating in open-loop tracking mode, such as Jason-3 and Sentinel-3, will deliver more observations, especially over mountainous regions.

Another solution is unmaned aearial vehicles (UAVs). Recent studies have shown the advantages of UAV-based altimetry over small rivers (Bandini et al., 2017a, 2017b). Due to its low-altitude flight, flexibility, and low cost, UAVs can potentially measure narrow rivers at very high spatial resolution at any time. This can complement the low coverage of satellite altimetry and fill the gap between spaceborne and ground-based observations.

### c. Water resources monitoring in the light of altimetry and imagery

Surface water storage dynamics can be more accurately quantified if dynamic water extent is available. In this regard, altimetry and imagery can be combined to measure water bodies in two dimensions, i.e. height and extent. This is also very important for 2D hydrodynamic modeling. The EU Copernicus programme simultaneously delivers imagery including both optical images (Sentinel-2) and SAR images (Sentinel-1), and altimetry data (CryoSat-2, Sentienl-3, Sentinel-6, etc.). This offers us opportunities to assess and predict condition and changes of water resources at high spatiotemporal resolution.

### d. Operational forecasting

Over the last several decades, remotely sensed hydrologic observations have been used for improving hydrologic predictions via model-data fusion. Several remote sensed variables, such as soil moisture, snow cover, terrestrial water storage, etc. have been successfully assimilated into models for forecasting purposes (Liu et al., 2012). Assimilating water surface elevation data retrieved from altimetry is not well explored, especially using data from geodetic altimetry missions. In a pioneering application (Schneider et al., 2018a), distributed WSE data was successfully assimilated into a 1D hydrodynamic model to improve discharge prediction. In the perspective of operational forecasting, developing a framework that can assimilate WSE from multiple altimetry missions can be helpful for flood forecasting and risk assessment. For example, ESA delivers near-real time Sentinel-3 L2 altimeter data within 3 hours and short-time critical data within 48 hours (European Space Agency, 2017), which can be put into play for flood forecasting.

# 8 References


Bakker, K., 2012. Water Security: Research Challenges and Opportunities. Science (80-. ). 337, 914–915. doi:10.1126/science.1226337

Bandini, F., Butts, M., Jacobsen, T.V., Bauer-Gottwein, P., 2017a. Water level observations from unmanned aerial vehicles for improving estimates of surface water-groundwater interaction. Hydrol. Process. 31, 4371–4383. doi:10.1002/hyp.11366

Bandini, F., Jakobsen, J., Olesen, D., Reyna-Gutierrez, J.A., Bauer-Gottwein, P., 2017b. Measuring water level in rivers and lakes from lightweight Unmanned Aerial Vehicles. J. Hydrol. 548, 237–250. doi:10.1016/j.jhydrol.2017.02.038

Bates, P.D., Pappenberger, F., Romanowicz, R.J., 2014. Uncertainty in Flood Inundation Modelling, in: Applied Uncertainty Analysis for Flood Risk Management. IMPERIAL COLLEGE PRESS, pp. 232–269. doi:10.1142/9781848162716_0010

Becker, M., Papa, F., Frappart, F., Alsdorf, D., Calmant, S., da Silva, J.S., Prigent, C., Seyler, F., 2018. Satellite-based estimates of surface water dynamics in the Congo River Basin. Int. J. Appl. Earth Obs. Geoinf. 66, 196–209. doi:10.1016/j.jag.2017.11.015

Berry, P.A.M., Garlick, J.D., Freeman, J.A., Mathers, E.L., 2005. Global inland water monitoring from multi-mission altimetry. Geophys. Res. Lett. 32, 1–4. doi:10.1029/2005GL022814

Biancamaria, S., Frappart, F., Leleu, A.-S., Marieu, V., Blumstein, D., Desjonquères, J.-D., Boy, F., Sottolichio, A., Valle-Levinson, A., 2017. Satellite radar altimetry water elevations performance over a 200m wide river: Evaluation over the Garonne River. Adv. Sp. Res. 59, 128–146. doi:10.1016/j.asr.2016.10.008

Biancamaria, S., Lettenmaier, D.P., Pavelsky, T.M., 2016. The SWOT Mission and Its Capabilities for Land Hydrology. Surv. Geophys. 37, 307–337. doi:10.1007/s10712-015-9346-y

Biancamaria, S., Schaedele, T., Blumstein, D., Frappart, F., Boy, F., Desjonquères, J.D., Pottier, C., Blarel, F., Niño, F., 2018. Validation of Jason-3 tracking modes over French rivers. Remote Sens. Environ. 209, 77–89. doi:10.1016/j.rse.2018.02.037

Birkett, C.M., 1995. The contribution of TOPEX/POSEIDON to the global monitoring of climatically sensitive lakes. J. Geophys. Res. 100, 25179. doi:10.1029/95JC02125

Birkinshaw, S.J., O'Donnell, G.M., Moore, P., Kilsby, C.G., Fowler, H.J., Berry, P.A.M., 2010. Using satellite altimetry data to augment flow estimation techniques on the Mekong River. Hydrol. Process. 24, 3811–3825. doi:10.1002/hyp.7811

Bjerklie, D.M., Dingman, S.L., Vorosmarty, C.J., Bolster, C.H., Congalton, R.G., 2003. Evaluating the potential for measuring river discharge from space. J. Hydrol. 278, 17–38. doi:10.1016/S0022-1694(03)00129-X

Bjerklie, D.M., Moller, D., Smith, L.C., Dingman, S.L., 2005. Estimating discharge in rivers using remotely sensed hydraulic information. J. Hydrol. 309, 191–209. doi:10.1016/j.jhydrol.2004.11.022

Carroll, M.L., Townshend, J.R., DiMiceli, C.M., Noojipady, P., Sohlberg, R. a., 2009. A new global raster water mask at 250 m resolution. Int. J. Digit. Earth 2, 291–308.

doi:10.1080/17538940902951401

CNES, 2016. SARAL / AltiKa Products Handbook.

Crétaux, J.-F., Abarca-del-Río, R., Bergé-Nguyen, M., Arsen, A., Drolon, V., Clos, G., Maisongrande, P., 2016. Lake Volume Monitoring from Space. Surv. Geophys. 37, 269–305. doi:10.1007/s10712-016-9362-6

Crétaux, J.F., Birkett, C., 2006. Lake studies from satellite radar altimetry. Comptes Rendus - Geosci. 338, 1098–1112. doi:10.1016/j.crte.2006.08.002

Dehecq, A., Gourmelen, N., Shepherd, A., Cullen, R., Trouvé, E., 2013. Evaluation of CryoSat-2 for height retrieval over the Himalayan range, in: CryoSat-2 Third User Workshop, March 2013. Dresden, Germany.

DHI, 2017. DHI simulation Engine for 1D river and urban modelling - Reference Mannual. DHI, Copenhagen.

Dingman, S., 2015. Physical hydrology, Third Edit. ed.

Domeneghetti, A., Tarpanelli, A., Brocca, L., Barbetta, S., Moramarco, T., Castellarin, A., Brath, A., 2014. The use of remote sensing-derived water surface data for hydraulic model calibration. Remote Sens. Environ. 149, 130–141. doi:10.1016/j.rse.2014.04.007

Durand, M., Gleason, C.J., Garambois, P.A., Bjerklie, D., Smith, L.C., Roux, H., Rodriguez, E., Bates, P.D., Pavelsky, T.M., Monnier, J., Chen, X., Di Baldassarre, G., Fiset, J.-M., Flipo, N., Frasson, R.P. d. M., Fulton, J., Goutal, N., Hossain, F., Humphries, E., Minear, J.T., Mukolwe, M.M., Neal, J.C., Ricci, S., Sanders, B.F., Schumann, G., Schubert, J.E., Vilmin, L., 2016. An intercomparison of remote sensing river discharge estimation algorithms from measurements of river height, width, and slope. Water Resour. Res. 52, 4527–4549. doi:10.1002/2015WR018434

European Space Agency, 2017. Sentinel-3 User Handbook.

European Space Agency, Mullar Space Science Laboratory, 2012. CryoSat Product Handbook.

Finsterle, S., Kowalsky, M.B., 2011. A truncated Levenberg-Marquardt algorithm for the calibration of highly parameterized nonlinear models. Comput. Geosci. 37, 731–738. doi:10.1016/j.cageo.2010.11.005

Floodlist, 2016. China [WWW Document].

Gao, H., He, X., Ye, B., Pu, J., 2012. Modeling the runoff and glacier mass balance in a small watershed on the Central Tibetan Plateau, China, from 1955 to 2008. Hydrol. Process. 26, 1593–1603. doi:10.1002/hyp.8256

Gao, L., Liao, J., Shen, G., 2013. Monitoring lake-level changes in the Qinghai–Tibetan Plateau using radar altimeter data (2002–2012). J. Appl. Remote Sens. 7, 073470. doi:10.1117/1.JRS.7.073470

Getirana, A.C. V., Boone, A., Yamazaki, D., Mognard, N., 2013. Automatic parameterization of a flow routing scheme driven by radar altimetry data: Evaluation in the Amazon basin. Water Resour. Res. 49, 614–629. doi:10.1002/wrcr.20077

Getirana, A.C. V, Bonnet, M.P., Calmant, S., Roux, E., Rotunno Filho, O.C., Mansur, W.J., 2009. Hydrological monitoring of poorly gauged basins based on rainfall-runoff modeling and spatial altimetry. J. Hydrol. 379, 205–219.

doi:10.1016/j.jhydrol.2009.09.049

Getirana, A.C. V, Peters-Lidard, C., 2013. Estimating water discharge from large radar altimetry datasets. Hydrol. Earth Syst. Sci. 17, 923–933. doi:10.5194/hess-17-923-2013

Gupta, H. V., Kling, H., Yilmaz, K.K., Martinez, G.F., 2009. Decomposition of the mean squared error and NSE performance criteria: Implications for improving hydrological modelling. J. Hydrol. 377, 80–91. doi:10.1016/j.jhydrol.2009.08.003

Hwang, C., Cheng, Y.-S., Han, J., Kao, R., Huang, C.-Y., Wei, S.-H., Wang, H., 2016. Multi-Decadal Monitoring of Lake Level Changes in the Qinghai-Tibet Plateau by the TOPEX/Poseidon-Family Altimeters: Climate Implication. Remote Sens. 8, 446. doi:10.3390/rs8060446

Kang, S., Xu, Y., You, Q., Flügel, W.-A., Pepin, N., Yao, T., 2010. Review of climate and cryospheric change in the Tibetan Plateau. Environ. Res. Lett. 5, 15101. doi:10.1088/1748-9326/5/1/015101

Kouraev, A. V., Zakharova, E.A., Samain, O., Mognard, N.M., Cazenave, A., 2004. Ob' river discharge from TOPEX/Poseidon satellite altimetry (1992–2002). Remote Sens. Environ. 93, 238–245. doi:10.1016/j.rse.2004.07.007

Lei, Y., Yao, T., Bird, B.W., Yang, K., Zhai, J., Sheng, Y., 2013. Coherent lake growth on the central Tibetan Plateau since the 1970s: Characterization and attribution. J. Hydrol. 483, 61–67. doi:10.1016/j.jhydrol.2013.01.003

Leon, J.G., Calmant, S., Seyler, F., Bonnet, M.-P., Cauhopé, M., Frappart, F., Filizola, N., Fraizy, P., 2006. Rating curves and estimation of average water depth at the upper Negro River based on satellite altimeter data and modeled discharges. J. Hydrol. 328, 481–496. doi:10.1016/j.jhydrol.2005.12.006

Lettenmaier, D.P., Alsdorf, D., Dozier, J., Huffman, G.J., Pan, M., Wood, E.F., 2015. Inroads of remote sensing into hydrologic science during the WRR era. Water Resour. Res. 51, 7309–7342. doi:10.1002/2015WR017616

Liu, G., Schwartz, F.W., Tseng, K.-H., Shum, C.K., 2015. Discharge and water-depth estimates for ungauged rivers: Combining hydrologic, hydraulic, and inverse modeling with stage and water-area measurements from satellites. Water Resour. Res. 51, 6017–6035. doi:10.1002/2015WR016971

Liu, J., Chen, X., Zhang, J., Flury, M., 2009. Coupling the Xinanjiang model to a kinematic flow model based on digital drainage networks for flood forecasting. Hydrol. Process. 23, 1337–1348. doi:10.1002/hyp.7255

Liu, Y., Weerts, A.H., Clark, M., Hendricks Franssen, H.-J., Kumar, S., Moradkhani, H., Seo, D.-J., Schwanenberg, D., Smith, P., van Dijk, A.I.J.M., van Velzen, N., He, M., Lee, H., Noh, S.J., Rakovec, O., Restrepo, P., 2012. Advancing data assimilation in operational hydrologic forecasting: progresses, challenges, and emerging opportunities. Hydrol. Earth Syst. Sci. 16, 3863–3887. doi:10.5194/hess-16-3863-2012

Ma, R., Duan, H., Hu, C., Feng, X., Li, A., Ju, W., Jiang, J., Yang, G., 2010. A half-century of changes in China's lakes: Global warming or human influence? Geophys. Res. Lett. 37.

Marquardt, D.W., 1963. An Algorithm for Least-Squares Estimation of Nonlinear Parameters. J. Soc. Ind. Appl. Math. 11, 431–441. doi:10.1137/0111030

Michailovsky, C.I., McEnnis, S., Berry, P. a M., Smith, R., Bauer-Gottwein, P., 2012. River monitoring from satellite radar altimetry in the Zambezi River basin. Hydrol. Earth Syst. Sci. 16, 2181–2192. doi:10.5194/hess-16-2181-2012

Neal, J.C., Odoni, N.A., Trigg, M.A., Freer, J.E., Garcia-pintado, J., Mason, D.C., Wood, M., Bates, P.D., 2015. Efficient incorporation of channel cross-section geometry uncertainty into regional and global scale flood inundation models. J. Hydrol. 529, 169–183. doi:10.1016/j.jhydrol.2015.07.026

Nielsen, K., Stenseng, L., Andersen, O.B., Knudsen, P., 2017. The Performance and Potentials of the CryoSat-2 SAR and SARIn Modes for Lake Level Estimation. Water 9, 374. doi:10.3390/w9060374

Nielsen, K., Stenseng, L., Andersen, O.B., Villadsen, H., Knudsen, P., 2015. Validation of CryoSat-2 SAR mode based lake levels. Remote Sens. Environ. 171, 162–170. doi:10.1016/j.rse.2015.10.023

Normandin, C., Frappart, F., Lubac, B., Bélanger, S., Marieu, V., Blarel, F., Robinet, A., Guiastrennec-Faugas, L., 2018. Quantification of surface water volume changes in the Mackenzie Delta using satellite multi-mission data. Hydrol. Earth Syst. Sci. 22, 1543–1561. doi:10.5194/hess-22-1543-2018

Paiva, R.C.D., Collischonn, W., Tucci, C.E.M., 2011. Large scale hydrologic and hydrodynamic modeling using limited data and a GIS based approach. J. Hydrol. 406, 170–181. doi:10.1016/j.jhydrol.2011.06.007

Pavlis, N.K., Holmes, S.A., Kenyon, S.C., Factor, J.K., 2012. The development and evaluation of the Earth Gravitational Model 2008 (EGM2008). J. Geophys. Res. Solid Earth 117, n/a-n/a. doi:10.1029/2011JB008916

Pekel, J.-F., Cottam, A., Gorelick, N., Belward, A.S., 2016. High-resolution mapping of global surface water and its long-term changes. Nature 1–19. doi:10.1038/nature20584

Pereverzyev, S.S., Pinnau, R., Siedow, N., 2006. Regularized fixed-point iterations for non-linear inverse problems. Inverse Probl. 22, 1–22. doi:10.1088/0266-5611/22/1/001

Qiu, J., 2008. The third pole. Nature 454, 393–396.

Rantz, S.E., 1982. Measurement and computation of streamflow: volume 2, computation of discharge. USGPO,.

Schneider, R., Godiksen, P.N., Villadsen, H., Madsen, H., Bauer-Gottwein, P., 2017. Application of CryoSat-2 altimetry data for river analysis and modelling. Hydrol. Earth Syst. Sci. 21, 751–764. doi:10.5194/hess-21-751-2017

Schneider, R., Ridler, M.E., Godiksen, P.N., Madsen, H., Bauer-Gottwein, P., 2018a. A data assimilation system combining CryoSat-2 data and hydrodynamic river models. J. Hydrol. 557, 197–210. doi:10.1016/j.jhydrol.2017.11.052

Schneider, R., Tarpanelli, A., Nielsen, K., Madsen, H., Bauer-Gottwein, P., 2018b. Evaluation of multi-mode CryoSat-2 altimetry data over the Po River against in situ data and a hydrodynamic model. Adv. Water Resour. 112, 17–26. doi:10.1016/j.advwatres.2017.11.027

Sichangi, A.W., Wang, L., Yang, K., Chen, D., Wang, Z., Li, X., Zhou, J., Liu, W., Kuria, D., 2016. Estimating continental river basin discharges using multiple remote sensing data sets. Remote Sens. Environ. 179, 36–53. doi:10.1016/j.rse.2016.03.019

Smith, L.C., Isacks, B., Bloom, A., 1996. Estimation of discharge from three braided rivers using synthetic aperture radar satellite imagery: Potential application to ungauged basins. Water Resour. Res. 32, 2021–2034. doi:10.1029/96WR00752

Snay, R.A., 2012. Evolution of NAD 83 in the United States: Journey from 2D toward 4D. J. Surv. Eng. 138, 161–171. doi:10.1061/(ASCE)SU.1943-5428.0000083

Song, C., Huang, B., Ke, L., 2015. Heterogeneous change patterns of water level for inland lakes in High Mountain Asia derived from multi-mission satellite altimetry. Hydrol. Process. 29, 2769–2781. doi:10.1002/hyp.10399

Sulistioadi, Y.B., Tseng, K.-H., Shum, C.K., Hidayat, H., Sumaryono, M., Suhardiman, A., Setiawan, F., Sunarso, S., 2015. Satellite radar altimetry for monitoring small rivers and lakes in Indonesia. Hydrol. Earth Syst. Sci. 19, 341–359. doi:10.5194/hess-19-341-2015

SWBD, 2003. Shuttle Radar Topography Mission Water Body Dataset [WWW Document]. URL https://lta.cr.usgs.gov/srtm_water_body_dataset (accessed 6.8.17).

Taube, C.M., 2000. Chapter 12: Three Methods for Computing the Volume of a Lake, in: Schneider, J.C. (Ed.), Manual of Fisheries Survey Mehtods II: With Periodic Updates. Michigan Department of Natural Resources.

Tonkin, M.J., Doherty, J., 2005. A hybrid regularized inversion methodology for highly parameterized environmental models. Water Resour. Res. 41, 1–16. doi:10.1029/2005WR003995

Tseng, K.H., Chang, C.P., Shum, C.K., Kuo, C.Y., Liu, K.T., Shang, K., Jia, Y., Sun, J., 2016. Quantifying freshwater mass balance in the central Tibetan Plateau by integrating satellite remote sensing, altimetry, and gravimetry. Remote Sens. 8. doi:10.3390/rs8060441

Villadsen, H., Andersen, O.B., Stenseng, L., Nielsen, K., Knudsen, P., 2015. CryoSat-2 altimetry for river level monitoring — Evaluation in the Ganges–Brahmaputra River basin. Remote Sens. Environ. 168, 80–89. doi:10.1016/j.rse.2015.05.025

Wilson, M., Bates, P., Alsdorf, D., Forsberg, B., Horritt, M., Melack, J., Frappart, F., Famiglietti, J., 2007. Modeling large-scale inundation of Amazonian seasonally flooded wetlands. Geophys. Res. Lett. 34. doi:10.1029/2007GL030156

Wingham, D.J., Francis, C.R., Baker, S., Bouzinac, C., Brockley, D., Cullen, R., de Chateau-Thierry, P., Laxon, S.W., Mallow, U., Mavrocordatos, C., Phalippou, L., Ratier, G., Rey, L., Rostan, F., Viau, P., Wallis, D.W., 2006. CryoSat: A mission to determine the fluctuations in Earth's land and marine ice fields. Adv. Sp. Res. 37, 841–871. doi:10.1016/j.asr.2005.07.027

Yan, K., Tarpanelli, A., Balint, G., Moramarco, T., Baldassarre, G., 2014. Exploring the Potential of SRTM Topography and Radar Altimetry to Support Flood Propagation Modeling: Danube Case Study. J. Hydrol. Eng. 20, 4014048. doi:10.1061/(ASCE)HE.1943-5584.0001018

Yanai, M., Li, C.F., 1994. Mechanism of Heating and the Boundary-Layer over the Tibetan Plateau. Mon. Weather Rev. doi:10.1175/1520-0493(1994)122<0305:MOHATB>2.0.CO;2

Yang, K., Ye, B., Zhou, D., Wu, B., Foken, T., Qin, J., Zhou, Z., 2011. Response of hydrological cycle to recent climate changes in the Tibetan Plateau. Clim. Change 109,

517–534. doi:10.1007/s10584-011-0099-4

Yang, R., Zhu, L., Wang, J., Ju, J., Ma, Q., Turner, F., Guo, Y., 2016. Spatiotemporal variations in volume of closed lakes on the Tibetan Plateau and their climatic responses from 1976 to 2013. Clim. Change 1–13. doi:10.1007/s10584-016-1877-9

Yao, T., Thompson, L.G., Mosbrugger, V., Zhang, F., Ma, Y., Luo, T., Xu, B., Yang, X., Joswiak, D.R., Wang, W., Joswiak, M.E., Devkota, L.P., Tayal, S., Jilani, R., Fayziev, R., 2012. Third Pole Environment (TPE). Environ. Dev. 3, 52–64. doi:10.1016/j.envdev.2012.04.002

Yuan, C., Gong, P., Zhang, H., Guo, H., Pan, B., 2017. Monitoring water level changes from retracked Jason-2 altimetry data: a case study in the Yangtze River, China. Remote Sens. Lett. 8, 399–408. doi:10.1080/2150704X.2016.1278309

Zhang, D., Zhang, L., Guan, Y., Chen, X., Chen, X., 2012. Sensitivity analysis of Xinanjiang rainfall–runoff model parameters: a case study in Lianghui, Zhejiang province, China. Hydrol. Res. 43, 123. doi:10.2166/nh.2011.131

Zhang, G., Xie, H., Kang, S., Yi, D., Ackley, S.F., 2011. Monitoring lake level changes on the Tibetan Plateau using ICESat altimetry data (2003-2009). Remote Sens. Environ. 115, 1733–1742. doi:10.1016/j.rse.2011.03.005

Zhao, R.-J., 1992. The Xinanjiang model applied in China. J. Hydrol. 135, 371–381. doi:10.1016/0022-1694(92)90096-E

Zheng, J., Ke, C., Shao, Z., Li, F., 2016. Monitoring changes in the water volume of Hulun Lake by integrating satellite altimetry data and Landsat images between 1992 and 2010. J. Appl. Remote Sens. 10, 016029. doi:10.1117/1.JRS.10.016029

Zhou, S., Kang, S., Chen, F., Joswiak, D.R., 2013. Water balance observations reveal significant subsurface water seepage from Lake Nam Co, south-central Tibetan Plateau. J. Hydrol. 491, 89–99. doi:10.1016/j.jhydrol.2013.03.030

# 9 Papers

**I** **Jiang, L.**, Schneider, R., Andersen, O. B., Bauer-Gottwein, P., "CryoSat-2 altimetry applications over rivers and lakes". *Water*, 2017, 9(3), 211.

**II** **Jiang, L.**, Nielsen, K., Andersen, O. B., Bauer-Gottwein, P., "Monitoring recent lake level variations on the Tibetan Plateau using CryoSat-2 SARIn mode data". *Journal of Hydrology*, 2017, 544, 109-124.

**III** **Jiang, L.**, Nielsen, K., Andersen, O. B., Bauer-Gottwein, P., "CryoSat-2 radar altimetry for monitoring freshwater resources of China". *Remote Sensing of Environment*, 2017, 200: 125-139.

**IV** **Jiang, L.**, Madsen, H., Bauer-Gottwein, P., "Calibration of river morphological parameters using satellite altimetry derived observations of water surface elevation". *In review.*

**TEXT FOR WWW-VERSION (with out papers)**

In this online version of the thesis, **paper I-IV** are not included but can be obtained from electronic article databases e.g. via www.orbit.dtu.dk or on request from.

DTU Environment
Technical University of Denmark
Miljoevej, Building 115
2800 Kgs. Lyngby
Denmark

info@env.dtu.dk.

The Department of Environmental Engineering (DTU Environment) conducts science based engineering research within five sections: Air, Land & Water Resources, Urban Water Systems, Water Technology, Residual Resource Engineering, Environmental Fate and Effect of Chemicals. The department dates back to 1865, when Ludvig August Colding gave the first lecture on sanitary engineering as response to the cholera epidemics in Copenhagen in the late 1800s.

**Department of Environmental Engineering**
Technical University of Denmark

DTU Environment
Bygningstorvet, building 115
2800 Kgs. Lyngby
Tlf. +45 4525 1600
Fax +45 4593 2850

www.env.dtu.dk